NUREG/CR-1335
EGG-2019

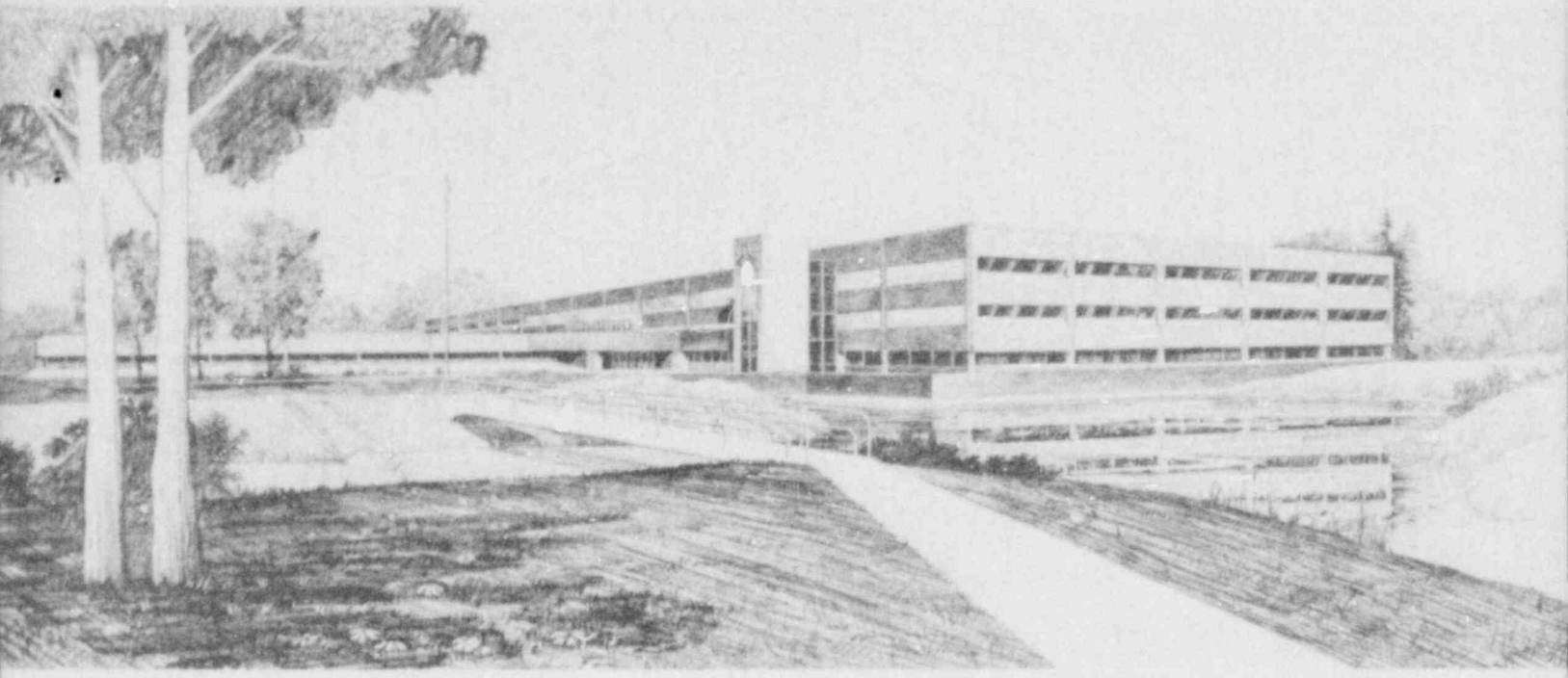

U.S. Department of Energy
Idaho Operations Office • Idaho National Engineering Laboratory

Irradiation Effects upon Selected Ceramic Cements and Ceramic Insulated Wires for Radiation-Resistant Transducers

Merlin E. Yancey
P. Victor Kelsey

April 1980

Prepared for the
U.S. Nuclear Regulatory Commission
Under DOE Contract No. DE-AC07-76IDO1570

EG&G Idaho

Available from

GPO Sales Program
Division of Technical Information and Document Control
U.S. Nuclear Regulatory Commission
Washington, D.C. 20555

and

National Technical Information Service
Springfield, Virginia 22161

NUREG/CR-1335
EGG-2019
Distribution Category:R2

IRRADIATION EFFECTS UPON SELECTED CERAMIC CEMENTS AND CERAMIC INSULATED WIRES FOR RADIATION-RESISTANT TRANSDUCERS

Merlin E. Yancey
P. Victor Kelsey

Published April 1980

EG&G Idaho, Inc.
Idaho Falls, Idaho 83415

Prepared for the
U.S. Nuclear Regulatory Commission
Washington, D.C. 20555
Under DOE Contract No. DE-AC07-76IDO1570
FIN No. A6048

ABSTRACT

Several high temperature ceramic cements and ceramic insulated wires were irradiated. The fast fluence ranged between 1.38 to 1.75 x 10^{20} nvt, and the thermal fluence ranged between 2.90 to 3.85 x 10^{20} nvt. Changes in the structural and bonding characteristics of the materials were noted. The evaluation indicated that most of the materials irradiated could be used in a nuclear environment.

CONTENTS

FIGURES

TABLES

SUMMARY

EG&G Idaho, Inc. has developed a number of special transducers which are subjected to high temperature, high pressure, and nuclear radiation. Material used in these transducers include ceramic insulated wire and high temperature ceramic cements. Since the manufacturers of these materials had only limited information on the materials' resistance to a radiation environment, an experiment was designed to evaluate the effects of nuclear radiation as well as the general structural and bonding characteristics of the irradiated ceramic material.

Test samples were prepared using small machinable ceramic and stainless discs coated with various ceramic cements, such as Ceramabond 503, Yellow Cerro, Sauereisen No. 8, Sauereisen No. 12, Dylon C-7, Dylon C-3 and Denex No. 2, and a ceramic flame sprayed material. Coils were also prepared using platinum, silver alloy, and gold wires. Changes in the inductance and resistance of the coils were recorded, as was the effect of irradiation on the ceramic insulation.

Flux monitors were used to determine the total irradiation to which the experiment was exposed. The fast fluence ranged between 1.38 to 1.75 x 10^{20} nvt, and the thermal fluence varied between 2.90 to 3.85 x 10^{20} nvt.

The irradiated ceramic cements showed no detectable change in their microstructure; however, some debonding and surface cracking occurred during irradiation. Several of the components fabricated from the machinable ceramic fractured during irradiation.

The irradiated coils showed an increase in electrical resistance while inductance remained essentially the same.

The electrical resistance of the platinum wire increased about 2.5%, while that of the silver alloy increased 9% and gold increased approximately 20% during irradiation. The insulation resistance on the silver alloy wire improved during irradiation.

IRRADIATION EFFECTS UPON SELECTED CERAMIC CEMENTS AND CERAMIC INSULATED WIRES FOR RADIATION-RESISTANT TRANSDUCERS

INTRODUCTION

EG&G Idaho, Inc., has developed a number of transducers to measure various phenomena associated with the Loss-of-Fluid Test (LOFT) Program. These transducers, which are used to measure the fluid density, velocity, and pressure, have been subjected to severe environments including nuclear radiation, high temperature, and high pressure.

High temperature corrosion resistant metals and inorganic materials such as ceramics, micas, and graphite are generally used in the design of these transducers because they exhibit good radiation resistance. Ceramic materials include high temperature ceramic cements, machinable ceramics, and ceramic insulated wires. The manufacturers of these materials had only limited information regarding the materials' resistance to a radiation environment. Therefore, an irradiation experiment was designed to simulate the nuclear environment experienced by the ceramic cements and the ceramic insulated wire during tests conducted as part of the LOFT Program. Other inorganic materials used in the fabrication of transducers were also irradiated as part of this experiment.

This report discusses the selection of materials which were irradiated, the experimental details, the preirradiation and the postirradiation examinations of the test samples, and a discussion of the results.

MATERIAL SELECTION

The design of ultrasonic, variable reluctance, and eddy current transducers fabricated by EG&G Idaho, Inc., employ small precision electronic coils. The materials used in the fabrication of these coils were irradiated in an experiment to identify possible irradiation damage. These coils were prepared on both ceramic and ceramic coated stainless steel coil forms using high temperature ceramic insulated platinum or silver alloy wires. Ceramic cements were then used to coat these coils and pot them in place. The ceramic cements presently being used in the fabrication of transducers include Sauereisen No. 8, Sauereisen No. 12, Ceramabond 503, and Yellow Cerro. Three other ceramic cements, Denex No. 2, Dylon C-3 and Dylon C-7, and a flame sprayed ceramic coating were also irradiated in this experiment.

Three other materials, phlogophite mica, graphite, and a machinable ceramic, used in various transducer designs were irradiated. The mica was used to provide a thin uniform insulating layer between a coil of ceramic insulated wire and a metallic surface. Coil forms were prepared from machinable ceramic material and graphite was used as a high temperature bearing material in transducers with rotating turbine blades.

In addition to EG&G-produced transducers, components of special transducers provided by Kaman Sciences Corporation for use in a high temperature nuclear environment were also irradiated. These components included special ceramic forms made of Kaman's K-ramic material, and two small coils prepared with ceramic insulated gold wire.

A complete list of irradiated materials and their suppliers is included in Appendix A.

EXPERIMENTAL DETAILS

The experiment consisted of three test capsules. The first two were filled with samples of various materials and the third with small test coils which were fabricated and coated with various cements. Numerous flux monitors were included in each capsule to obtain data on the thermal and fast flux irradiation levels accumulated during the experiment.

The experiment was irradiated in the Advanced Test Reactor during a 28-day cycle. The experiment's irradiation levels, based upon the expected irradiation level of the LOFT Program, is as follows:

Thermal: $5.6 \times 10^{18} - 5.6 \times 10^{20}$ nvt

Fast: $2.7 \times 10^{17} - 2.7 \times 10^{19}$ nvt

Since the primary purpose of the irradiation experiment was to evaluate the effects of irradiation on the ceramic cements and the electrical properties of the small coils prepared with ceramic insulated wire, the experimental details related to the graphite, mica, and other material included in the experiment will be discussed in Appendix B.

Test Samples

A series of test samples were designed to evaluate the structural characteristics of the various ceramic cements and ceramic coatings, including their capability to maintain a bond during irradiation to: (a) 304 stainless steel, (b) machinable ceramic material, and (c) other ceramic cements. The test samples consisted of small stainless steel and ceramic discs 1 mm thick with a diameter of 9.52 mm, each coated with either a single or double layer of cement. Each layer of cement was between 380 to 635μ thick.

A total of 40 stainless steel discs and 55 ceramic discs were prepared. The surfaces of all the stainless steel discs and 22 of the ceramic discs were sandblasted with a No. 40 aluminum oxide grit to roughen their surfaces so that the ceramic cements would adhere more tightly to them. Tables 1 and 2 identify the various samples with their coating. Where two cements were specified, the first was completely cured before the second cement was applied.

Additional test samples were designed to evaluate the effects of irradiation on the electrical parameters of coils, their resistance, inductance, and insulation resistance. Both 304 stainless steel and ceramic material were used to prepare coil forms as shown in Figure 1. The 304 stainless steel coil forms were sandblasted and flame sprayed with 50- to 100-μ coating of BLH Electronics Ceramic. All of the coil forms were labeled with permanent identification. Twenty-one coils were prepared in sets of three with approximately 150 to 160 windings each. Each set was wound with a 17.78 mm diameter ceramic insulated wire, and coated with the ceramic cement as indicated in Table 3.

TABLE 1. CERAMIC DISC EVALUATION SAMPLES

Sample Identification		
Control	Irradiated	Coatings
1, 1S[a]	1, 1, 1S[a]	Ceramabond 503
2, 2S	2, 2, 2S	Yellow Cerro
3, 3S	3, 3, 3S	Sauereisen No. 8
4, 4S	4, 4, 4S	Sauereisen No. 12
5, 5S	5, 5, 5S	Dylon C-7
6, 6S	6, 6, 6S	Denex No. 2
7, 7S	7, 7, 7S	Ceramabond 503 and Sauereisen No. 8
8, 8S	8, 8, 8S	Ceramabond 503 and Sauereisen No. 12
9, 9S	9, 9, 9S	Sauereisen No. 8 and Sauereisen No. 12
10, 10S	10, 10, 10S	Denex No. 2 and Dylon C-7
O, X(S)	O, Y, Z(S)	Dylon C-3

a. S indicates sample with sandblasted surface.

Three additional coils were prepared with approximately 120 bifilar windings of ceramic insulated wire and were used to determine irradiation effects on the insulation resistance of the Type E ceramic insulation. No ceramic cement was applied to these coils.

In preparing these test samples, all ceramic materials, ceramic cements, and the Type E insulation were cured according to the manufacturer's specification.

Capsules and Test Assembly

Three test capsules of varying lengths were designed using 304 stainless steel tubing with an outer diameter of 1.27 cm and a 0.889 mm wall thickness. Stainless steel end plugs were welded into each end of the capsule. Capsule A contained

TABLE 2. STAINLESS STEEL EVALUATION SAMPLES

Sample Identification		
Control	Irradiated	Coatings
A, A	A, A, A	Flame Sprayed Ceramic
1, 1	1, 1, 1	Ceramabond 503
2, 2	2, 2, 2	Yellow Cerro
3, 3	3, 3, 3	Sauereisen No. 8
4, 4	4, 4, 4	Sauereisen No. 12
5, 5	5, 5, 5	Dylon C-7
6, 6	6, 6, 6	Denex No. 2
10, 10	7, 8, 8	Dylon C-3

the transducer components supplied by Kaman Sciences Corporation and samples of mica. Capsule B contained all of the ceramic cement samples and three small graphite disc samples. The 24 test coils were contained in Capsule C. Each of the test capsules contained a series of flux monitors for determining the amount of fast and thermal flux the samples were exposed to during irradiation. These three capsules were sealed within a larger single capsule having an outer diameter of 1.59 cm and a 1.24 mm wall thickness to provide double containment of the experiment. The double containment was required to meet the reactor safety requirements since the experiment contained both gold and silver. Each containment boundary met the American Society of Mechanical Engineers' (ASME), Section III, Class I equivalent requirements. The doubly contained experiment, and a small aluminum screw top capsule containing additional flux monitor materials were placed in a Y-basket fixture for insertion into the reactor's experiment irradiation facilities. Details of the capsules and test assembly are shown Appendix C.

Test Condition

The experiment was not designed to provide actual temperature data during irradiation. Therefore, engineering calculations were made in order to estimate the maximum expected centerline temperature during irradiation. An analysis based on a realistic gamma heat generation of 16W/g yielded a maximum centerline temperature of 437K during irradiation.

The various flux monitors included in the experiment were evaluated to determine the irradiation levels accumulated during the experiment. The fast fluence (>1 MeV relative to U_{235}) were determined from the ^{54}Fe (n,p)^{54} Mn reaction assuming a reactor cross section of 68 millibarns. The fast fluence ranged between 1.38 to 1.75 x 10^{20} nvt. The thermal fluences (2200 m/s) were determined from the ^{59}Co (n,γ)^{60}Co reaction assuming a reactor cross section of 37.2 barns and ranged between 2.90 to 3.85 x 10^{20} nvt. The estimated errors on these flux measurements are $\pm$15% (1σ). Appendix D contains a detailed tabulation of the irradiation levels accumulated during the experiment.

PREIRRADIATION EXAMINATION

Prior to irradiation, detailed photographs were taken of all the samples and test coils. The general structural conditions of each of the samples and test coils were noted and recorded. Before sealing, the test samples and coils were heated to 672K for 25 hours to ensure complete drying.

Ceramic Cements

In order to better understand the bonding mechanism and the composition of the various ceramic cements, a qualitative spectrographic analysis of the ceramic cements and test discs was performed. The results are shown in Table 4. The specific phases present in the ceramic cements were determined by X-ray diffraction analysis and are listed in Table 5.

From the preceding analysis it can be determined that with the exception of Dylon C-3 and C-7, the ceramic cements are "phosphate" bonded with various included aggregates, the coarser aggregates being those phase identified in the X-ray diffraction analysis. (Phosphate bonding is essentially a chemical reaction which yields long phosphate chains held together by alkali or small alkaline earth ions.)

The Dylon C-3 and C-6 cements are probably silicate bonded as indicated by the presence of a

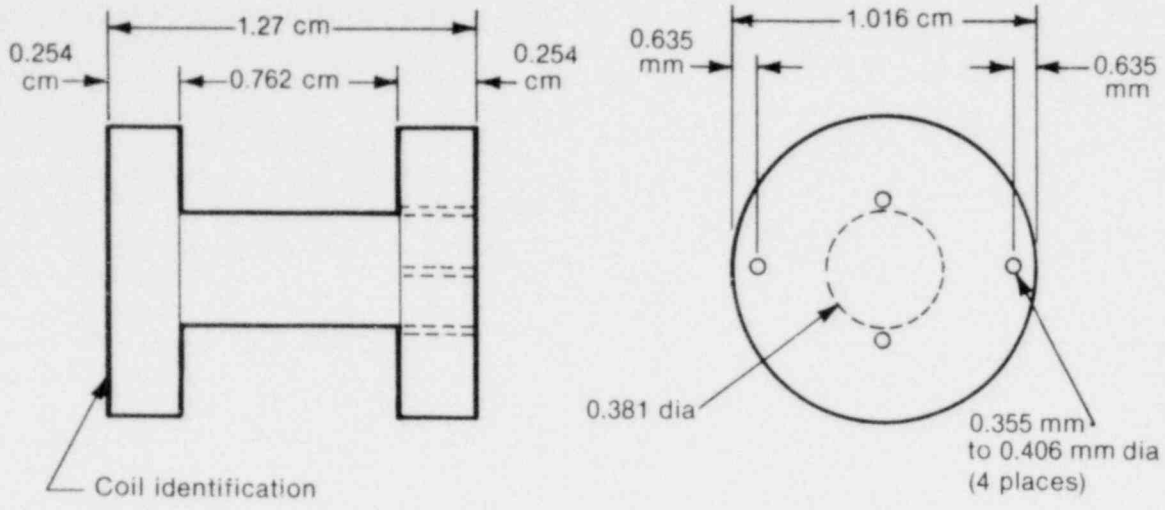

A. Machinable ceramic coil form

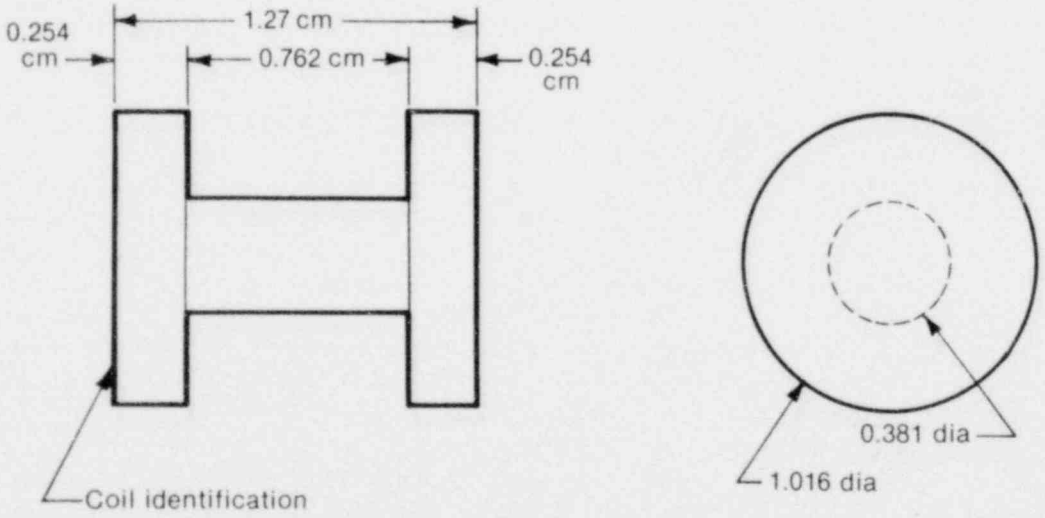

B. 304 stainless steel coil form

INEL-A-14 810

Figure 1. Schematic drawing of coil forms.

TABLE 3. TEST COIL IDENTIFICATION

Identification	Coil Form	Wire	Coating
1A, 1B, 1C	304 SS	Alloy 406	Ceramabond 503
2A, 2B, 2C	Ceramic	Alloy 406	Ceramabond 503
3A, 3B, 3C	Ceramic	Alloy 406	Ceramabond 503 and Sauereisen No. 8
4A, 4B, 4C	Ceramic	Alloy 406	Yellow Cerro
5A, 5B, 5C	Ceramic	Alloy 406	Denex No. 2
6A, 6B, 6C	Ceramic	Alloy 406	Dylon C-7
7A, 7B, 7C	Ceramic	Platinum	Ceramabond 503
A, B, C	Ceramic	Alloy 406	No coating, bifilar wound

TABLE 4. QUALITATIVE SPECTROGRAPHIC ANALYSIS[a]

Elements	Aremcolox 502-1100	Denex No.2	Dylon C-3	Dylon C-7	Sauereisen No.8	Sauereisen No. 12	Ceramabond 503	Yellow Ce.ro
Ag	VF	VF	VVF	VVF	VF	VF+		VVF
Al	VS	S	ST	VS	ST	ST	VS	S
B	FT	FT	VF	VF	ST	FT	T	ST
Ba	FT+	FT			FT			FT
Ca	T+	ST	FT	T	ST	T+	T	ST
Cr	T	ST+	T	T	VF	VF	FT	S
Fe	T+	FT+	T	T	T	T	T	FT+
Mg	T	T	FT	ST	S	S	FT	FT
P	T	VS	S		VS	VS	VS	VS
Si	VS	VS	VS	S+	VS	VS	ST	VS
Ti	ST	S+	T+		T+	T	VF+	FT
Zr	ST	ST	FT		VS	S+	FT	FT
Na	ST	T	S	S	FT	FT	T	T+
K	ST	T	T	S	FT	FT	T	T
Li	FT	VF	VF	FT	VF	VF	VF+	VF+

Symbol	PPM-Range	Symbol	%Range
VVF	1	T	0.01-0.1
VVF+	0.5-5	T+	0.05-0.5
VF	1-10	ST	0.1-1.0
		ST+	0.5-5
VF+	5-50	S	1-10
FT	10-100	S+	5-50
FT+	50-500	VS	10-100

a. Analysis by GTE Sylvania, Towanda, Pennsylvania.

TABLE 5. PHASES PRESENT IN THE CERAMIC CEMENTS

Cements	Phases
Denex No. 2	α - Quartz, TiO_2 (Rutile)
Dylon C-3	α - Quartz, Glass
Dylon C-7	Al_2O_3, Glass
Sauereisen No. 8	Zircon ($ZrSiO_4$)
Sauereisen No. 12	Zircon ($ZrSiO_4$)
Ceramabond 503	Al_2O_3
Yellow Cerro	α - Quartz

glass phase in the X-ray analysis coupled with a low or undetectable phosphorous content. (Silicate bonded cements are generally formed by the dehydration of hydrous alkali silicates which have extremely low melting points. The dehydration process results in an amorphous glassy phase which acts as a "hardened glue" about various aggregates by forming silicate chains upon dehydration.)

X-ray diffraction of the Aremcolox 502-1100 machinable ceramic was inconclusive due to its highly complicated structure. The material utilized for the ceramic disc, and ceramic coil forms, is probably a multiphase ceramic composed of various Al_2O_3-SiO_2 minerals in a glass matrix.

The samples' general condition was observed, including their surface texture and cracking. Photographs and photomicrographs of the test samples were prepared to record their preirradiated condition. These photographs showing the eight basic coatings are included in Appendix E. Dylon C-3 and Sauereisen 8 cements had a grainy texture while the other cements and coatings had a fine texture. Dylon C-7 was a fine textured cement; however, the coating as applied was rough in appearance with several surface cracks.

In all the samples where two ceramic coatings were applied to a single base material, the coatings appeared to bond very well to each other.

The samples were heated to 672K while being prepared for packaging. The samples were removed while the oven was still at temperature; the removal resulted in a thermal shock. Due to the differences in the thermal expansion rates of the ceramic coatings and the stainless steel disc, and the quality of the bonding mechanism, debonding occurred between Sauereisen No. 12, Ceramabond 503, and the 304 stainless steel discs to which they were coated.

Ceramic Insulated Wire

The preirradiated condition of the test coils with the various ceramic coatings is also shown in Appendix E. The two small coils supplied by Kaman Sciences Corporation are not shown. They were fabricated with a ceramic insulated gold wire. The general appearance of all the ceramic cements on the coils was similar to the condition of the basic cement samples. Some surface cracking occurred in Sauereisen 8, Yellow Cerro, and Dylon C-7.

The electrical resistance and inductance of each of the coils was measured using a Hewlett-Packard LCR meter (HP-4262) with a 10 kHz test signal. The insulation resistance of the three bifilar wound coils was measured with a Hewlett-Packard high resistance meter (HP-4329A). The electrical resistance, inductance, and insulation resistance of the various coils were recorded to determine the effects of irradiation on these parameters.

POSTIRRADIATION EXAMINATION

The postirradiation examination of the irradiated cements and coils included a visual examination of the general condition of each sample, and a photomicrograph of each type of sample to identify change in the microstructure of the samples.

Ceramic Cements

Figure 2 shows photographs of the irradiated ceramic discs with various cement coatings. The condition of the irradiated stainless steel discs which were coated with ceramic cements is shown in Figure 3. Table 6 identifies the various irradiated cement samples and provides a brief summary of sample condition after irradiation. In general, all of the cements maintained their bond to the ceramic discs with the exception of Dylon C-3. Five of the ceramic discs fractured during irradiation. The Yellow Cerro cement

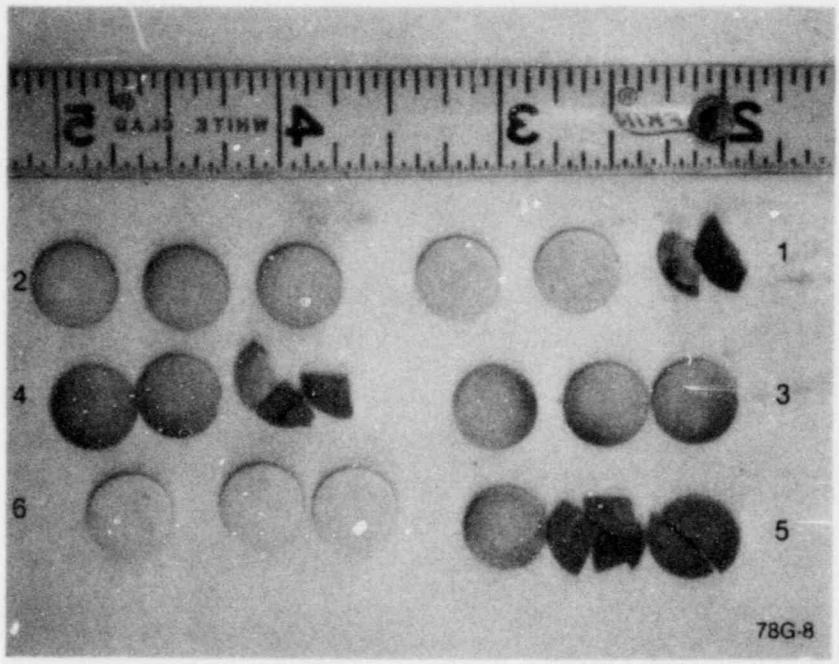

(a)

(b)

GS-017-001

Figure 2. Condition of irradiated ceramic discs with various cement coatings.

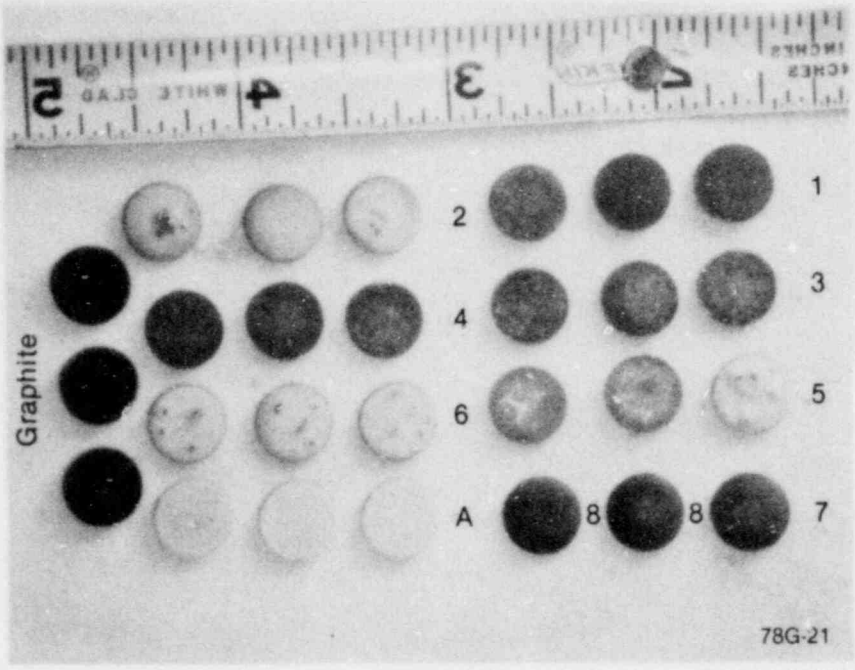

GS-017-002

Figure 3. Irradiated graphite and stainless steel discs showing irradiated condition. Debond between stainless steel and cement occurred on samples 1, 3, 4, 5, 7, 8.

TABLE 6. SUMMARY OF VISUAL INSPECTION AFTER IRRADIATION

Identification	Disc	Coatings	Visual Inspection of Irradiated Samples (3 each)
1	Ceramic	Ceramabond 503	Smooth surface; no cracking; one broken disc
2	Ceramic	Yellow Cerro	Smooth surface; hairline cracks
3	Ceramic	Sauereisen No. 8	Roughness similar to preirradiated condition; no cracking; dark pepper-like grains on surface
4	Ceramic	Sauereisen No. 12	Roughness similar to preirradiated condition; no cracking; one broken disc
5	Ceramic	Dylon C-7	Two broken discs; cracking similar to preirradiated condition
6	Ceramic	Denex No. 2	Smooth surface; no cracking
7	Ceramic	Ceramabond 503 and Sauereisen No. 8	All appeared acceptable
8	Ceramic	Ceramabond 503 and Sauereisen No. 12	All appeared acceptable
9	Ceramic	Sauereisen Nos. 8 and 12	All appeared acceptable
10	Ceramic	Denex No. 2 and Dylon C-7	All appeared acceptable
Z, O, Y	Ceramic	Dylon C-3	One broken disc; cement debond occurred on all three samples
A	304 SS	Flame Spray	Fine textured surface;similar to preirradiated condition
1	304 SS	Ceramabond 503	Cement debond occurred prior to irradiation as a result of thermal shock
2	304 SS	Yellow Cerro	All appeared acceptable; fine cracks in surface on two samples
3	304 SS	Sauereisen No. 8	Cement debond had occurred
4	304 SS	Sauereisen No. 12	Cement debond occurred prior to irradiation as a result of thermal shock
5	304 SS	Dylon C-7	One sample acceptable; debond had occurred in two samples; surface cracks
6	304 SS	Denex No. 2	No cracks; fine textured surface; all look good
7, 8, 8	304 SS	Dylon C-3	Debond had occurred on all three samples

developed some additional hairline cracks during irradiation. Only three of the coatings maintained their bonds to the 304 stainless steel discs during irradiation. These included Denex No. 2, Yellow Cerro, and the flame sprayed coating. Yellow Cerro had developed some fine hairline cracks on the surface, while the surface condition of both Denex No. 2 and the flame sprayed coating appeared similar to preirradiation samples.

Microscopic examination of the irradiated samples was undertaken to offer possible cause and effect relationships for the macroscopic behavior of various cements and to evaluate their bonding characteristics. The photomicrographs of the irradiated samples are presented in Appendix F. These photomicrographs show that the cement on four of the six irradiated ceramic samples maintained an excellent bond during irradiation. The photomicrographs of the Dylon C-7 and the Sauereisen No. 8 cements showed a thin layer of mounting epoxy appearing in the region of the former bonds indicating the bonds' deterioration. All samples with two layers of cement coated on them showed that these cements adhered very well to each other. Coatings which adhered to the stainless steel discs following the original curing process, also maintained their bond during irradiation. The basic microscopic structure of all the samples appeared unaffected by irradiation.

Two additional tests were conducted on the ceramic discs which had a single layer of ceramic cement. In the first of these tests, the coatings were scraped with a sharp instrument to determine whether the irradiated coatings were hard or soft. The Yellow Cerro and a sample Dylon C-7 on a small piece of ceramic material were soft and could be scraped from a ceramic disc. Ceramabond 503, Denex No. 2, Sauereisen No. 8, and Sauereisen No. 12 all appeared very hard. Five test samples were then intentionally broken to see if this would result in a debonding of the cement coating from the ceramic discs. The five ceramic coatings maintained their bonds to the ceramic discs as they were broken. Suitable samples of Dylon C-3 and Dylon C-7 were not available for this test.

Ceramic Insulated Wire

The general condition of the coil prepared with the ceramic insulated wire was noted. Four of the coil forms fractured during irradiation, including all three of the coils coated with the Yellow Cerro cements. The coils coated with Yellow Cerro showed some surface cracking upon irradiation. The three coils wound on the flame sprayed stainless steel forms and coated with Ceramabond 503 showed some surface cracking with the coating on one of the coils actually flaking off the windings. Photographs showing the condition of the various coils as they were removed from the capsules after irradiation are shown in Appendix G.

Resistance and inductance measurements on the irradiated coils were made and compared with the preirradiated data. These resistance and inductance values are tabulated in Table 7. (Table 3 provides additional coil identification information.)

The electrical resistance of all the coils increased as a result of irradiation. The largest increase in resistance, approximately 20%, occurred in the Kaman coils prepared with gold wire. An average increase of about 9% in electrical resistance occurred in the coils wound with the Alloy 406 (silver alloy) wire, while an increase of 2.5% occurred in the platinum wire. All inductance changes were generally less than $\pm 1\%$ of the preirradiated values.

The insulation resistance of the irradiated Secon Type E insulation was measured and compared with the preirradiated data. The insulation resistance on each of the bifilar wound coils was measured and recorded as shown in Table 8. The windings of one of the coils shorted during irradiation, and the other two coils showed a substantial increase in insulation resistance during irradiation.

Metallographic analysis of the coil wires before and after irradiation (metallographs shown in Appendix H) indicates a marked increase in the number and average size of voids within the metal after irradiation. The effect is especially pronounced in the silver (Alloy 406) wire, in which the average void size increased from 3.6×10^{-4} mm to 3.6×10^{-3} mm, and the number of voids increased by a factor greater than 3.5. While the effects of irradiation upon the gold and platinum wires is not as dramatically evident, there is an increase in the number and average void size after irradiation.

TABLE 7. TEST DATA ON THE COILS BEFORE AND AFTER IRRADIATION

Identification	Condition[a]	Resistance (Ohms)	Inductance (Microhenries)	Identification	Condition[a]	Resistance (Ohms)	Inductance (Microhenries)
1A	U	13.97	62.3	5A	U	14.64	69.0
	I	15.12	65.2		I	16.08	69.4
1B	U	14.09	63.7	5B	U	14.38	66.8
	I	15.62	63.2		I	16.03	67.3
1C	U	13.88	60.8	5C	U	14.34	66.3
	I	14.69	61.7		I	17.60	66.6
2A	U	14.37	66.3	6A	U	14.72	68.7
	I	15.30	66.8		I	Lead broke	Lead broke
2B	U	14.36	66.1	6B	U	14.83	69.6
	I	15.29	66.6		I	15.69	69.7
2C	U	14.36	65.8	6c	U	14.74	68.6
	I	15.79	66.5		I	15.71	68.8
3A	I	14.72	68.4	7A	U	12.21	64.5
	I	15.99	68.6		I	12.51	64.8
3B	U	14.45	67.1	7B	U	12.32	65.3
	I	15.62	67.2		I	12.63	65.6
3C	U	14.43	66.7	7C	U	12.46	68.2
	I	15.72	67.0		I	12.65	68.5
4A	U	14.33	66.1	Kaman No. 1	U	8.90	15.27
	I	15.69	64[b]		I	10.77	15.23
4B	U	14.56	68.6	Kaman No. 2	U	8.94	15.56
	I	16.12	68.2[b]		1	11.34	15.52
4C	U	14.24	65.3				
	I	16.05	63.8[b]				

a. U-Unirradiated; I-Irradiated.

b. Coil pulled apart.

TABLE 8. INSULATION RESISTANCE DATA

Identification	Insulation Resistance	
	Preirradiated	Irradiated
A	0.95×10^9 ohms	1.5×10^9 ohms
B	0.3×10^9 ohms	12.23 ohms
C	0.65×10^9 ohms	1.65×10^9 ohms

DISCUSSION AND CONCLUSIONS

Ceramic Cement Behavior

From the examination of the coated discs and the fabricated coils before and after irradiation, it was determined that Denex No. 2 cement was superior to the other cements tested in the maintenance of the bond to both ceramic and metallic substrates. The improved properties of this phosphate bonded cement may be the result of a TiO_2 (rutile) aggregate addition. In general, the phosphate bonded cements adhered to the ceramic and metal discs better than those cements which utilized the silicate bond. The cement-to-cement bonds appeared to be unaffected by the irradiation. Several of the ceramic discs and coil forms fabricated from the Aremcolox Machinable Ceramic 502-1100 fractured during irradiation. The microstructure of the cements, coil forms, and other investigated materials appeared unaffected by the irradiation.

In general, all of the ceramic cements with the exception of the silicate bonded cements could be recommended for use in a nuclear environment. It should be kept in mind that some of the cements would be better suited for designs requiring an encased potting because of debond and cracking, while other cements like Denex No. 2 and Yellow Cerro could be used in a variety of applications.

Ceramic Insulated Wire Behavior

The increase in the electrical resistivity of the coils as a result of irradiation can be explained by considering the atomistic effects of irradiation upon the wire. The irradiation, via fast or thermal neutrons, of the wire (in this case gold, silver alloy, or platinum) will result in atoms being knocked from their crystallographic positions. Subsequent collisions occur as the neutron continues along its path, and as the struck atom is propelled, a damage cascade is produced. The degree of absorption (or probability of collision) will be directly related to the neutron capture cross section of the material. As a result of the damage, the crystal structure is disrupted and the mean free path for electron transport is shortened. Therefore, an increase can be expected in the resistivity proportional to the neutron capture cross section. The thermal neutron activation cross section in barns (isomeric and ground state), σ_γ, for gold, silver, and platinum is (0 + 98.8), $\sim$(3 + 62.1), and $\sim$(0.04 + 10.1) respectively. The increases in resistivity of 20, 9, and 2.5% for the above wires are approximately proportional to the cross sections for these elements.

The microstructure of the silver alloy was affected by the radiation to a much greater extent than that of gold or platinum. The mechanism for the large void growth which occurred during irradiation is not explained at this time.

The insulation resistance of the Secon Type E insulation increased as a result of irradiation. This increase resulted from structural changes in the insulation similar to the changes that caused an increase in the electrical resistance of the wire that was irradiated.

Inductance, which is more dependent upon coil geometry and design rather than electrical properties, was unaffected by the irradiation.

Both platinum and the silver alloy wire with the Type E insulation could be recommended for use in nuclear environments. Platinum wire should be considered for applications which require a high degree of accuracy, while the silver alloy wire could be used in less critical applications. For instance, silver alloy wire could be used in transducers designed for use with electronic bridge circuits and applications.

APPENDIX A

MATERIALS LIST

APPENDIX A

MATERIALS LIST

The following is a list of suppliers and their materials used in the irradiation experiment.

Ceramic Cements and Coatings:

Trade Name	Supplier
Sauereisen No. 8	Sauereisen Cement Co., Pittsburgh, PA
Sauereisen No. 12	Sauereisen Cement Co., Pittsburgh, PA
Ceramabond 503	Aremco Products Inc., Ossining, NY
Yellow Cerro	Hi-Tec Corporation, Westford, MA
Denex No. 2	Dentronics, Inc., Hackensack, NY
Dylon C-3	Dylon Industries, Cleveland, OH
Dylon C-7	Dylon Industries, Cleveland, OH
Flame Sprayed Ceramic Coating 215020 BLH-H	BLH Electronics, Waltham, MA

Other Materials:

Material	Supplier
Phlogophite Mica	Asheville-Schoonmaker Mica Co., Newport News, VA
Aremcolox Machinable Ceramic 502-1100	Aremco Products Inc., Ossining, NY
Graphite Type RCH658	Pure Carbon Co., St. Marys, PA
Platinum Wire with Type E Ceramic Insulation	Secon Metals Corporation, White Plains, NY
K-Ramic Material and Transducer Components	Kaman Sciences Corp., Colorado Springs, CO

APPENDIX B

IRRADIATION EFFECTS ON TRANSDUCER COMPONENTS

APPENDIX B

IRRADIATION EFFECTS ON TRANSDUCER COMPONENTS

Several transducer components were irradiated as part of this experiment in order to evaluate their use in nuclear radiation applications. The specific items of interest included mica, graphite, machinable ceramic, and some small ceramic transducer components supplied by Kaman Sciences Corporation.

The following items were prepared and included in the irradiation experiment:

1. Four phlogophite mica discs, 0.00254 cm x 0.698 cm in diameter
2. Three graphite discs, 0.127 cm x 0.952 cm diameter
3. Coil forms and discs fabricated using a machinable ceramic
4. Kaman transducer components including four K-ramic line guides (10 mm), two ceramic transducer components, and two small coils.

The location of the various items within the experiment capsules can be seen in the figures of Appendix C.

The approximate irradiation levels seen by the various components can be determined from data reported in Appendix D.

The condition of the irradiated contents of Capsule A which included the components supplied by Kaman as well as the mica and the machinable ceramic can be seen in Figure B-1. No apparent physical damage occurred to the small coils, the transducer components, or the mica during irradiation; however, half of both the machinable ceramic items and the line guides fractured during irradiation.

The general condition of the irradiated graphite discs can be seen in Figure 3. The graphite maintained structural integrity during irradiation.

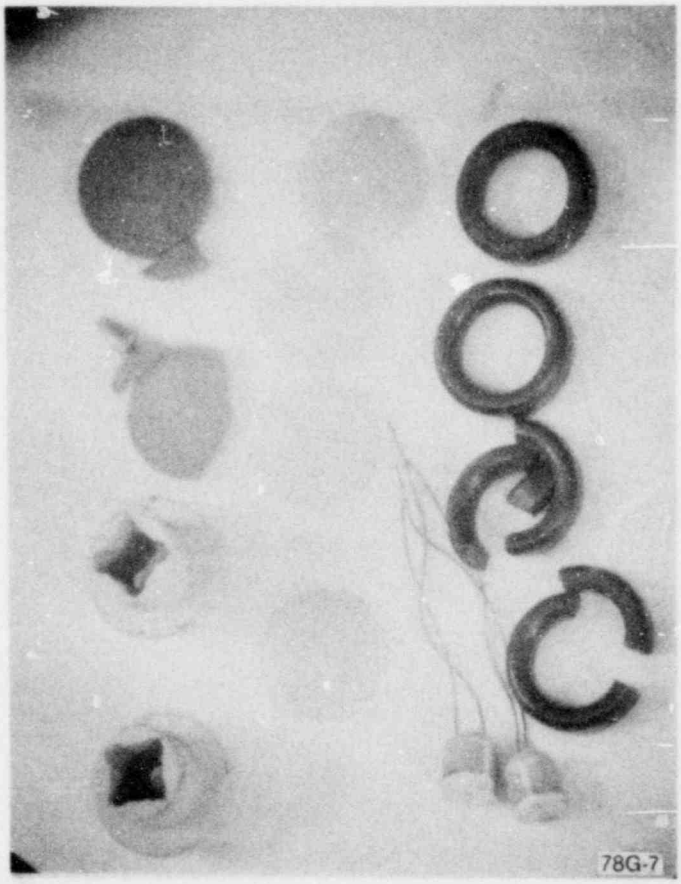

GS-017-003

Figure B-1. Irradiated contents of capsule A including ceramic transducer components (2 each),machinable ceramic (2 each), mica (4 each), Kaman coils (2 each), and ceramic line guides (4 each).

APPENDIX C

DETAILS OF CAPSULES AND TEST ASSEMBLIES

APPENDIX C

DETAILS OF CAPSULES AND TEST ASSEMBLIES

The dimensions of Capsules A and B, as well as capsule content are shown in the sketches of Figure C-1. Figure C-2 shows the locations of the various coils included in Capsule C. The locations of the flux monitor within the various capsules are shown in Figures C-1 and C-2.

The final arrangement of the capsules relative to each other and their location in the Y-Basket are shown in Figure C-3.

The Y-Baskets were designed specifically for loading the experiment into the Advanced Test Reactor's B-hole irradiation facility.

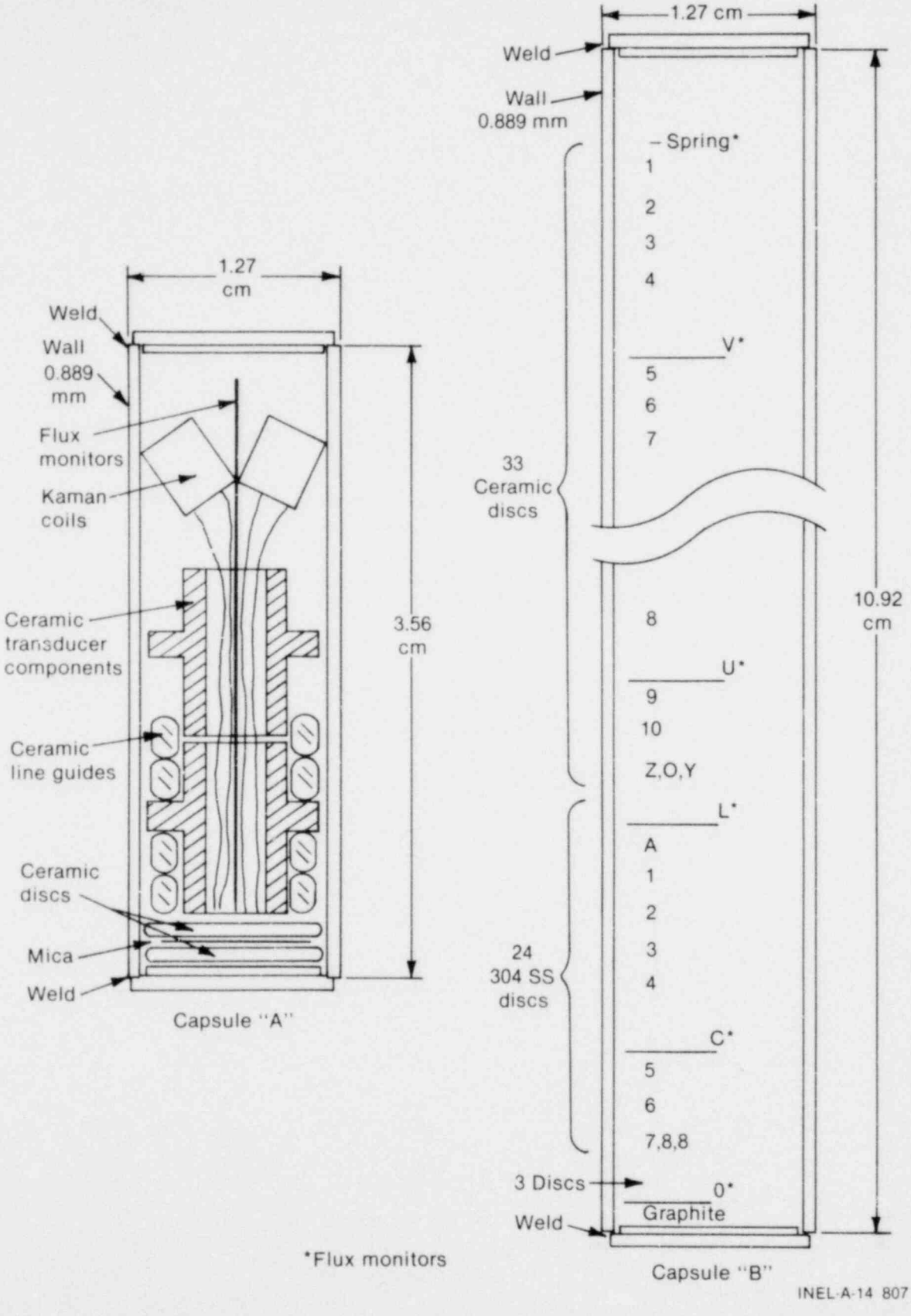

Figure C-1. Sketches of capsules A and B showing the capsules contents.

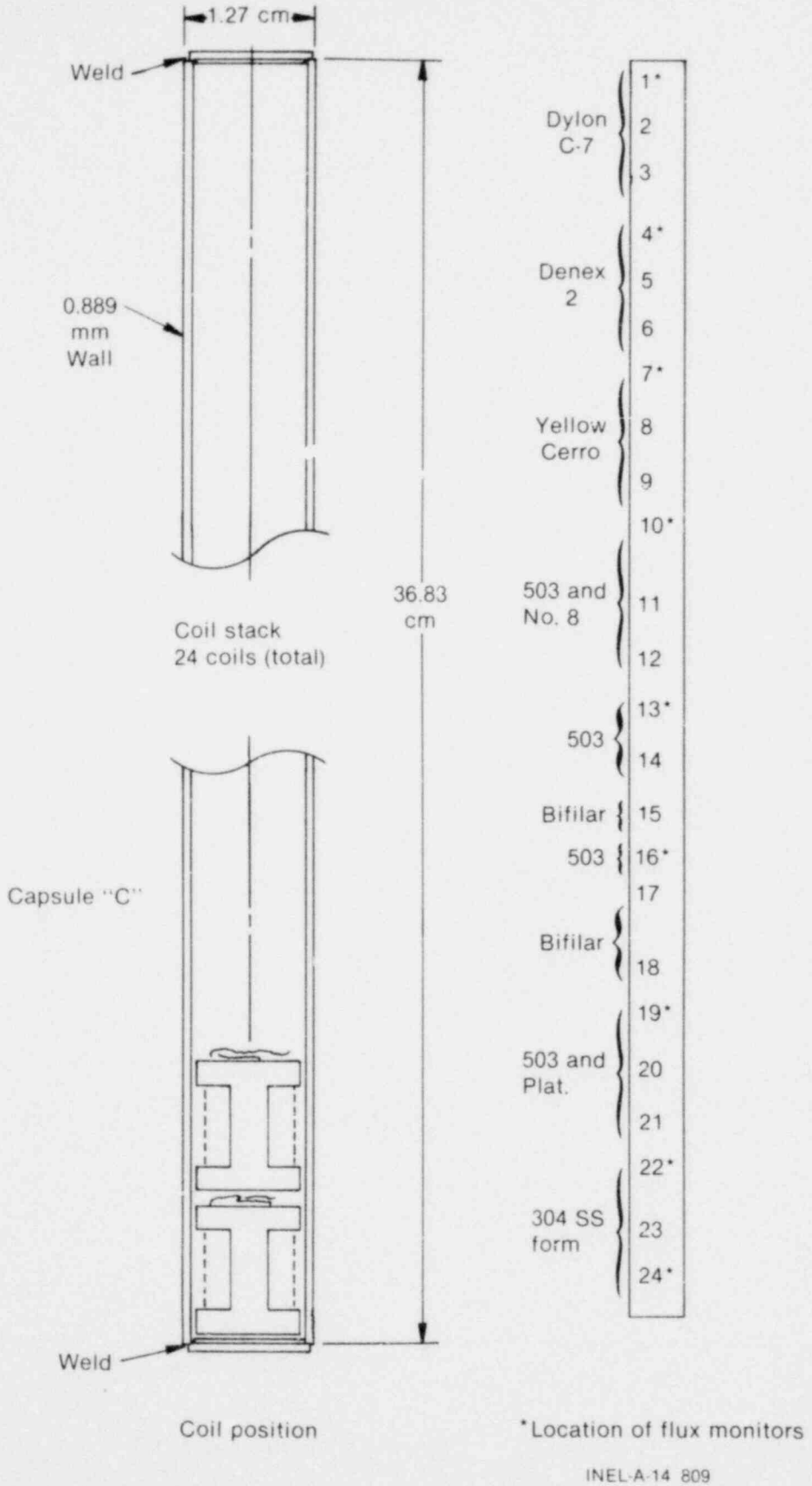

Figure C-2. Sketch of capsule C showing location of coils.

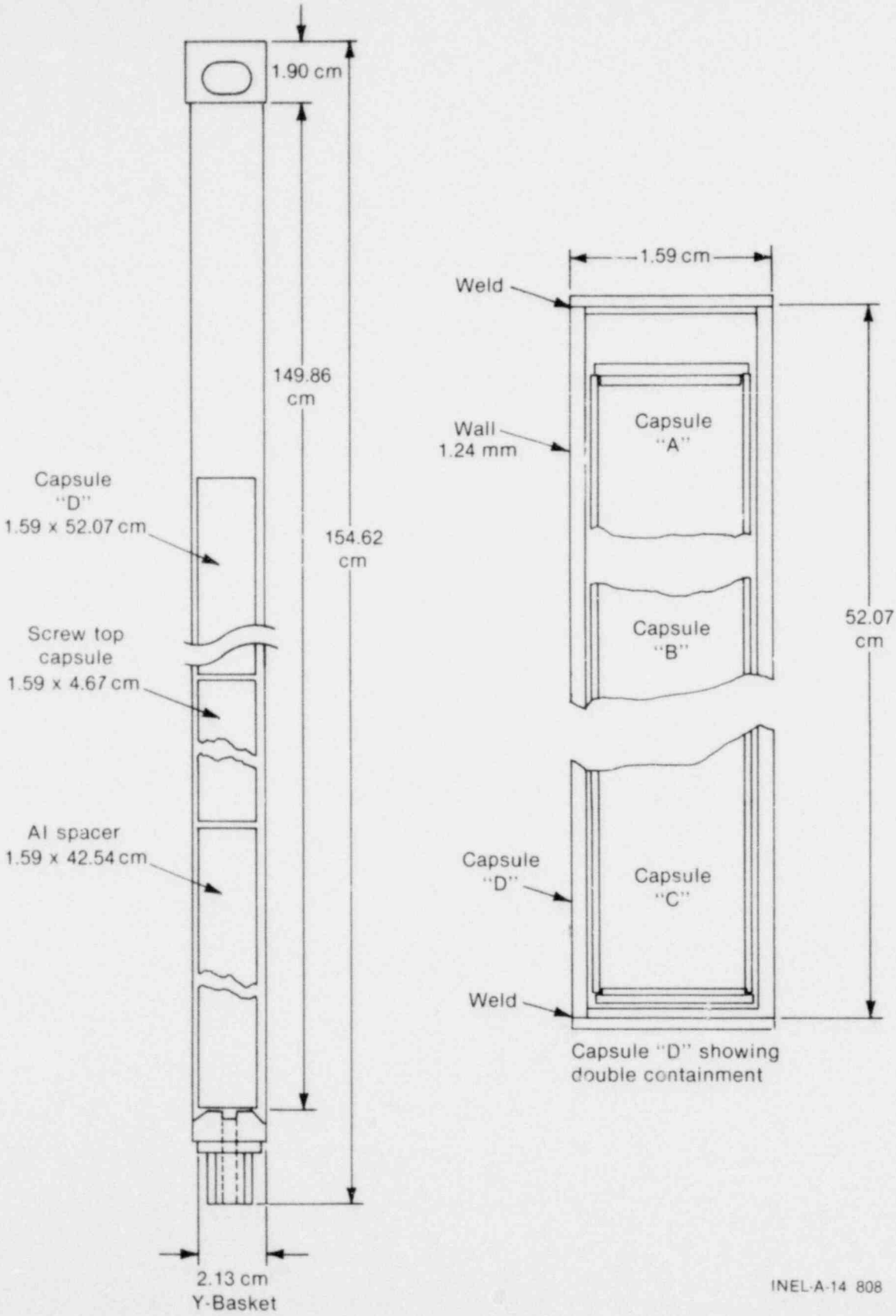

Figure C-3. Capsule arrangement within capsule D and the Y-Basket.

APPENDIX D

IRRADIATION LEVELS ACCUMULATED DURING THE EXPERIMENT

APPENDIX D

IRRADIATION LEVELS ACCUMULATED DURING THE EXPERIMENT

Table D-1 contains a tabulation of fast neutron data, and Table D-2 contains a tabulation of the thermal neutron data obtained from evaluating the various flux monitors. The location of the various monitors within the experiment is shown in the sketches of Appendix C.

TABLE D-1. FAST NEUTRON IRRADIATION DATA

Capsule	Monitor	Fast Flux (>1 MeV nv)	Fast Fluence (>1 MeV nvt)
A	Top	6.48×10^{13}	1.57×10^{20}
A	Center	6.47	1.56
A	Bottom	6.50	1.57
B	V	6.71	1.62
B	U	6.84	1.65
B	L	6.70	1.62
B	C	6.49	1.57
B	O	6.79	1.64
C	1	7.12	1.72
C	4	7.28	1.76
C	7	7.18	1.73
C	10	7.25	1.75
C	13	7.23	1.75
C	16	7.10	1.72
C	19	6.94	1.68
C	22	6.83	1.65
C	24	6.30	1.52
2	2	5.70	1.38

TABLE D-2. THERMAL NEUTRON IRRADIATION DATA

Capsule ID	Monitor ID	Thermal Flux (2200 m/s nv)	Thermal Fluence (2200 m/s nvt)
A	Top	1.29×10^{14}	3.12×10^{20}
A	Center	1.29	3.12
A	Bottom	1.20	2.90
B	V	1.34	3.24
B	U	1.34	3.24
B	L	1.33	3.21
B	C	1.30	3.14
B	O	1.36	3.29
C	1	1.39	3.36
C	4	1.36	3.29
C	7	1.35	3.26
C	10	1.34	3.24
C	13	1.33	3.22
C	16	1.40	3.39
C	19	1.36	3.29
C	22	1.26	3.05
C	24	1.22	2.95
2	2	1.59	3.85

APPENDIX E

PREIRRADIATED SAMPLES AND TEST COILS

APPENDIX E

PREIRRADIATED SAMPLES AND TEST COILS

The general condition of each of the basic coatings on the preirradiated samples can be seen in Figures E-1 to E-4. The base material to which each of the ceramic cements were applied consisted of three stainless steel discs (the upper three samples of each set) and three ceramic discs. The flame sprayed ceramic coating was applied to only three stainless steel discs.

Figure E-5 shows the preirradiated condition of the 24 coils prepared for the experiment.

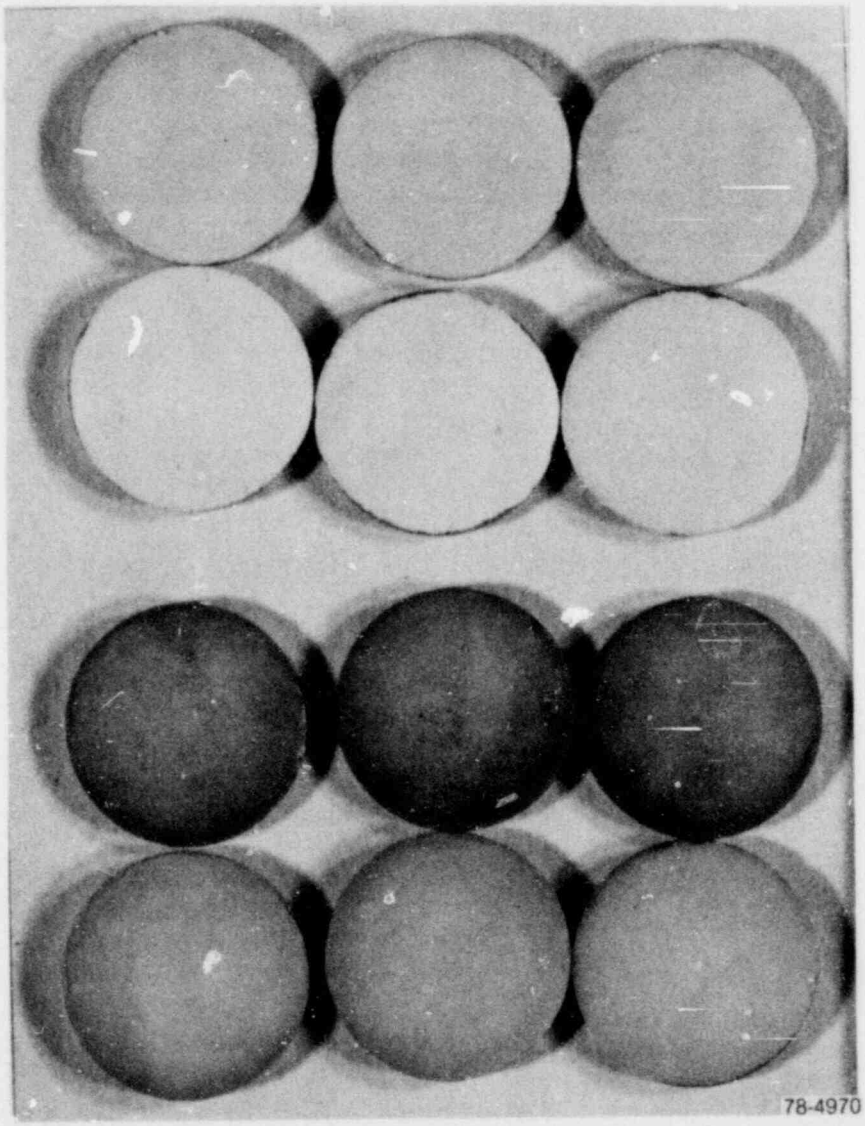

Figure E-1. Preirradiated Denex No. 2 and Yellow Cerro samples.

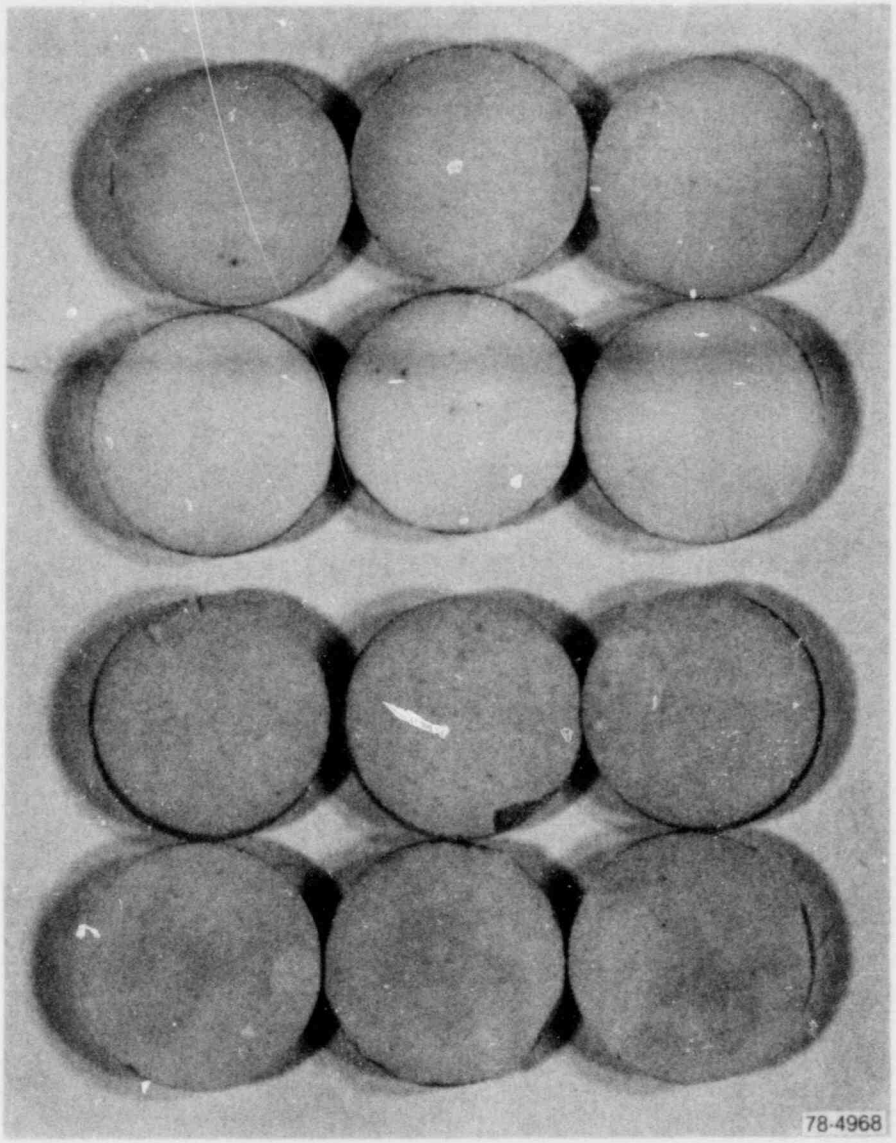

GS-017-019

Figure E-2. Preirradiated Ceramabond 503 and Sauereisen No. 12 samples.

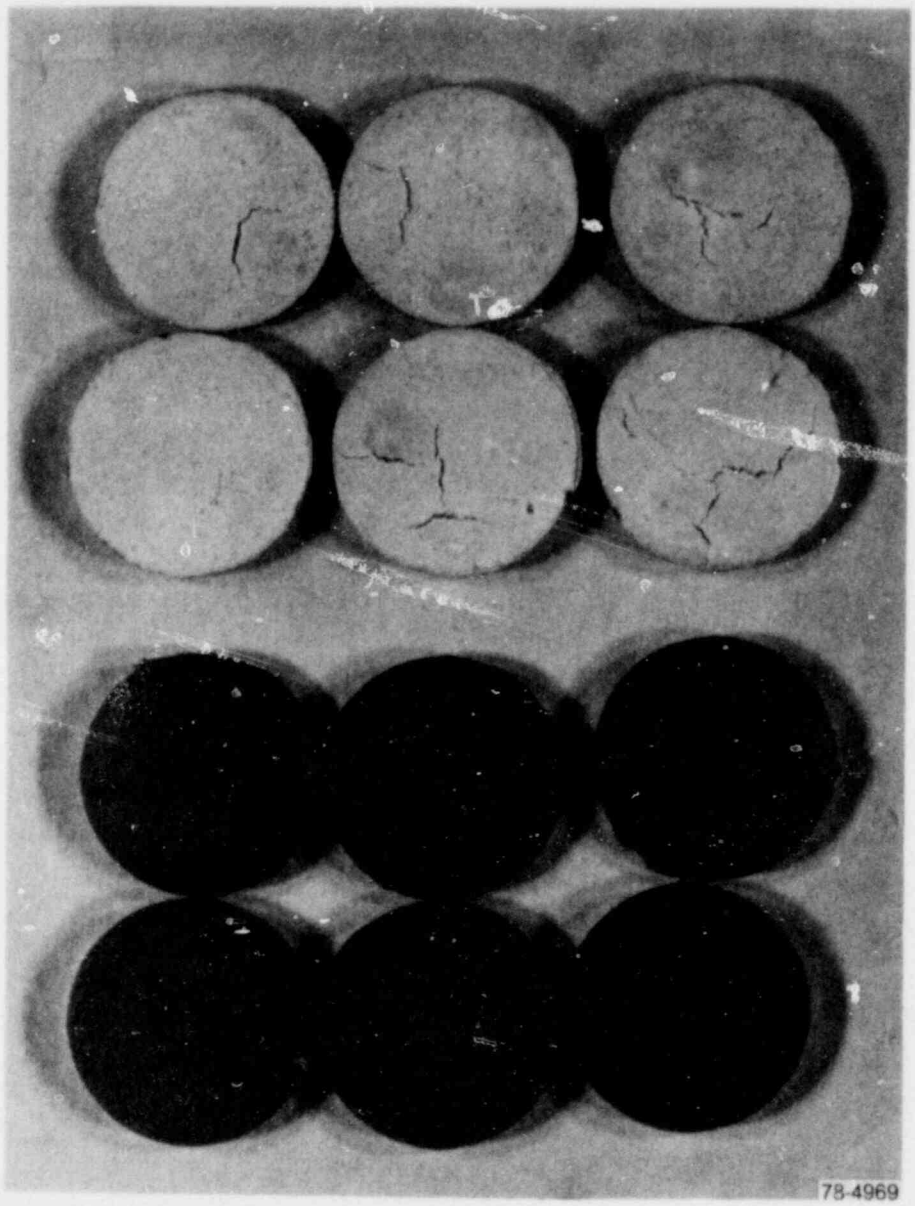

Figure E-3. Preirradiated Dylon C-7 and Dylon C-3 samples.

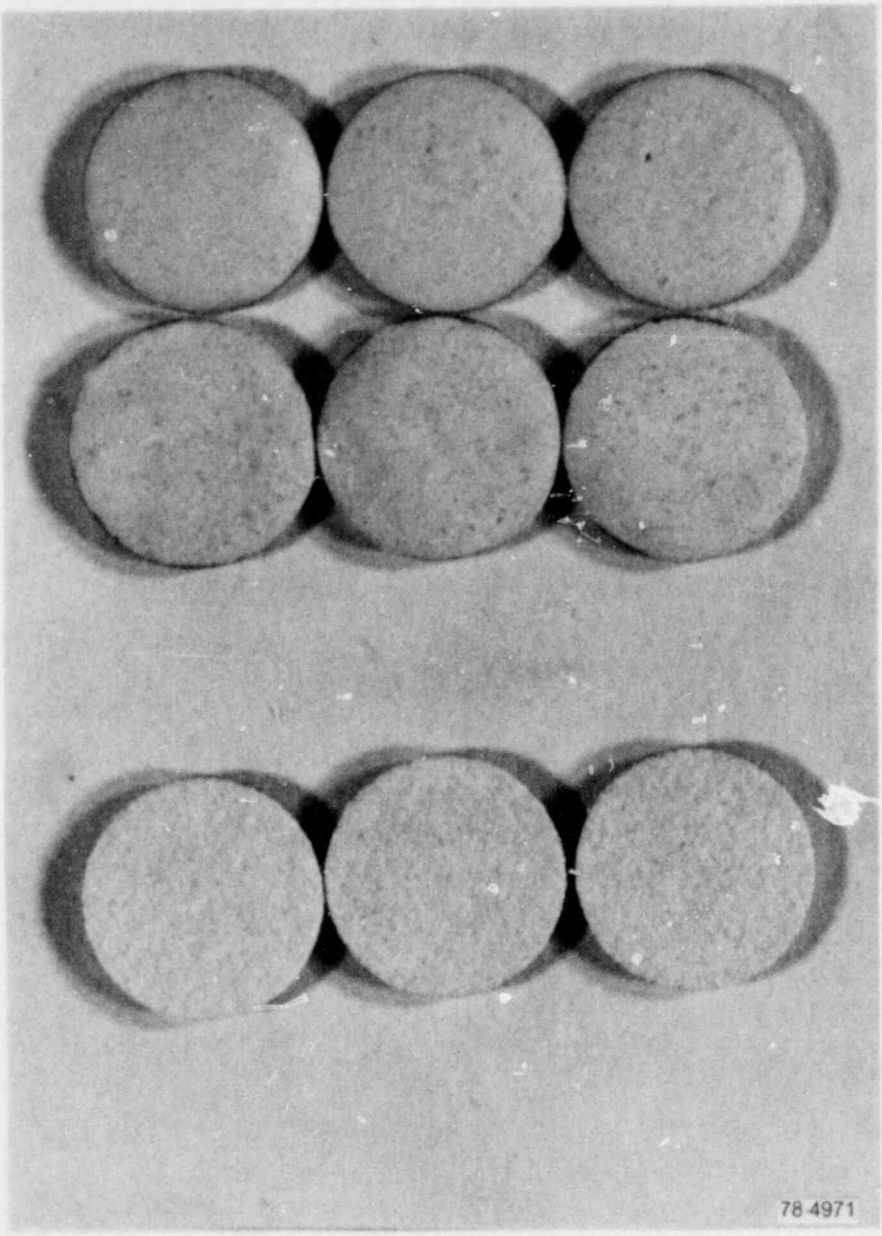

GS-017-021

Figure E-4. Preirradiated Sauereisen No. 8 and Flame Sprayed Samples.

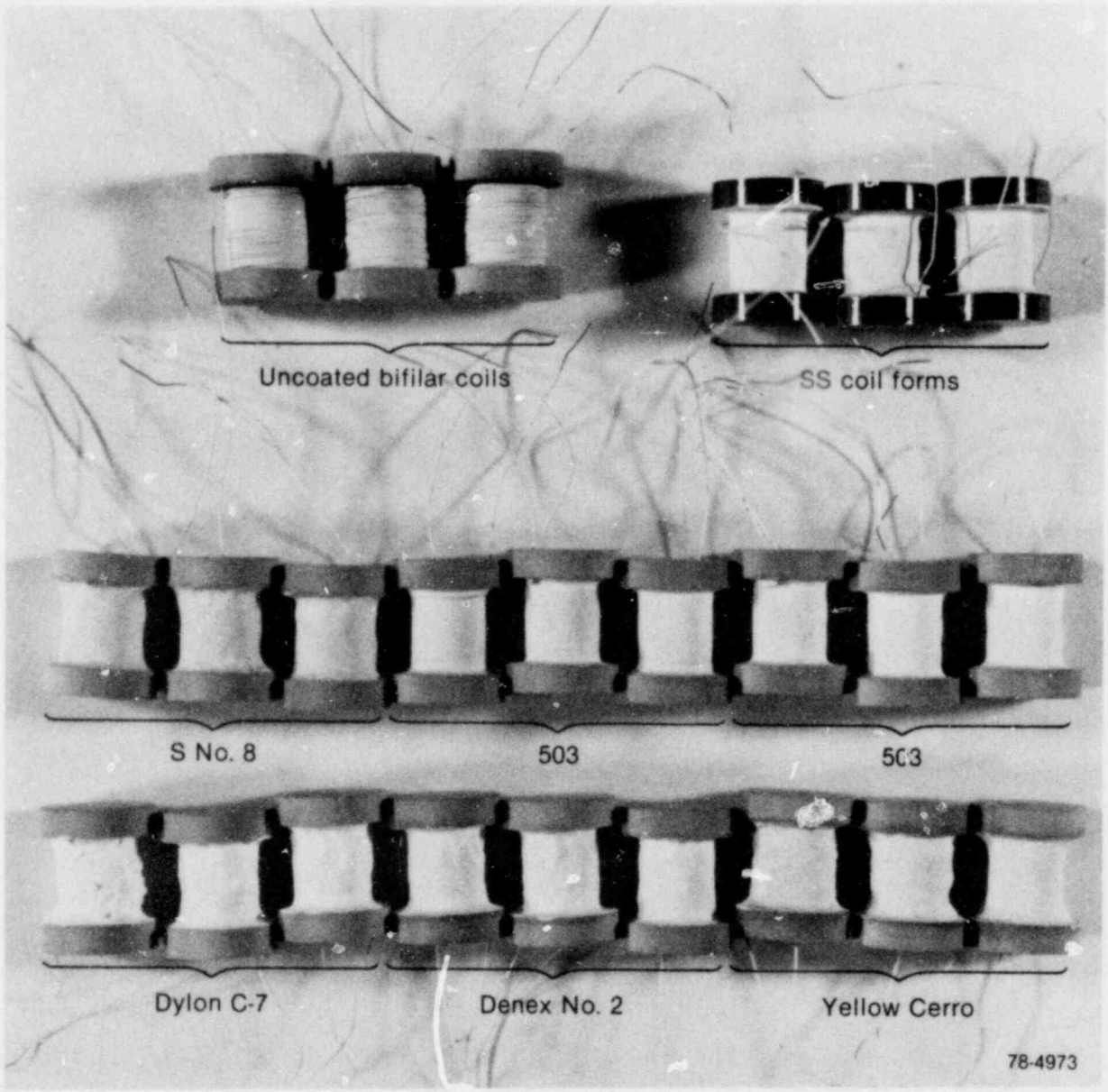

GS-017-022

Figure E-5. Preirradiated condition of the test coils.

APPENDIX F

PHOTOMICROGRAPHS OF IRRADIATED SAMPLES

APPENDIX F

PHOTOMICROGRAPHS OF IRRADIATED SAMPLES

Photomicrographs showing details of the bond between the ceramic discs and the ceramic cements are shown in Figures F-1 through F-6. Debonding had occurred on all samples coated with Dylon C-3.

Figures F-7 through F-10 show cross sections of the ceramic discs with two layers of ceramic cements.

A cross section of the four samples which maintained their bond to the stainless steel discs is shown in Figures F-11 to F-14.

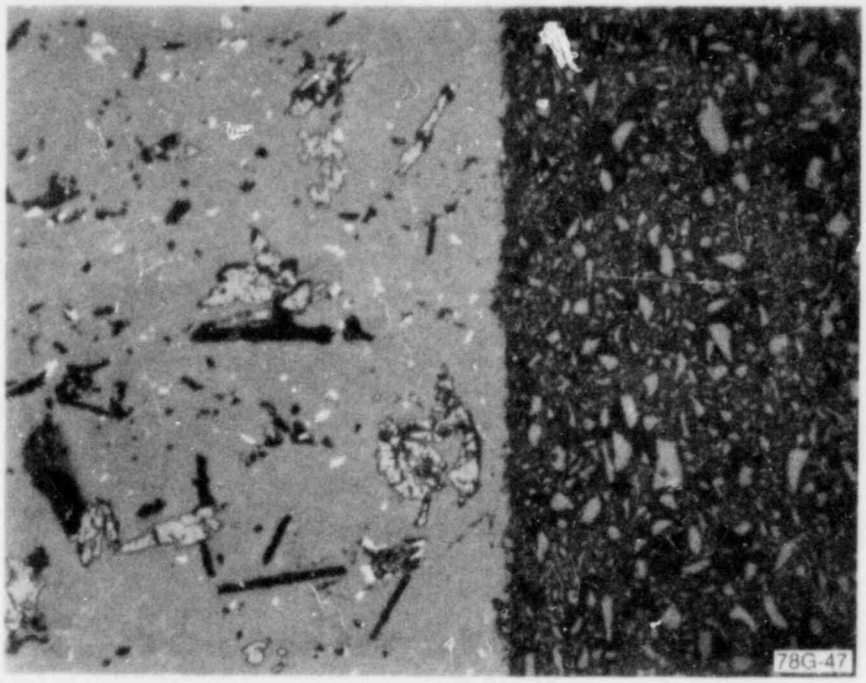

Figure F-1. Interface of ceramic disc with Yellow Cerro after irradiation (200X).

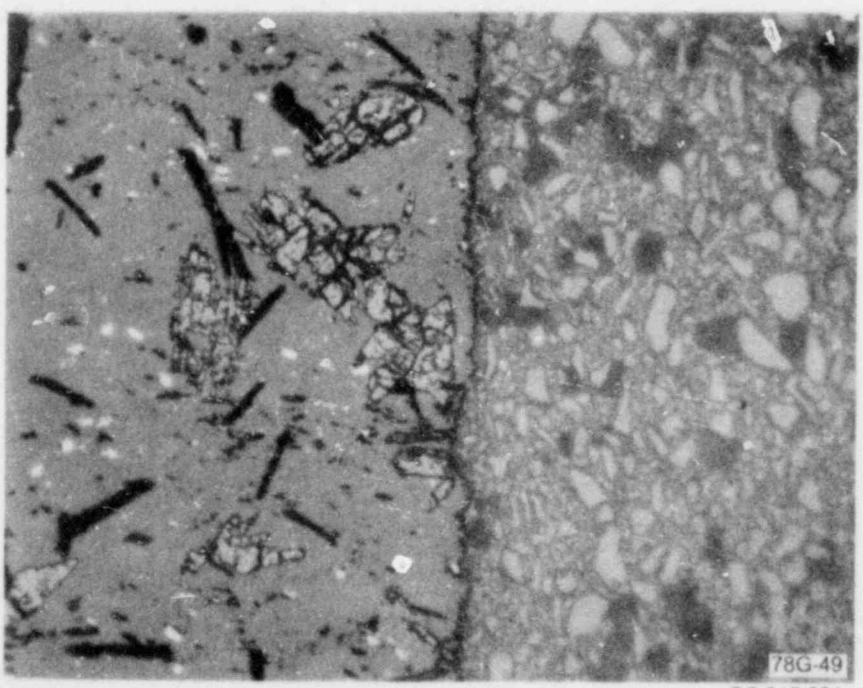

GS-017-004

Figure F-2. Interface of ceramic disc with Denex No. 2 after irradiation (200X).

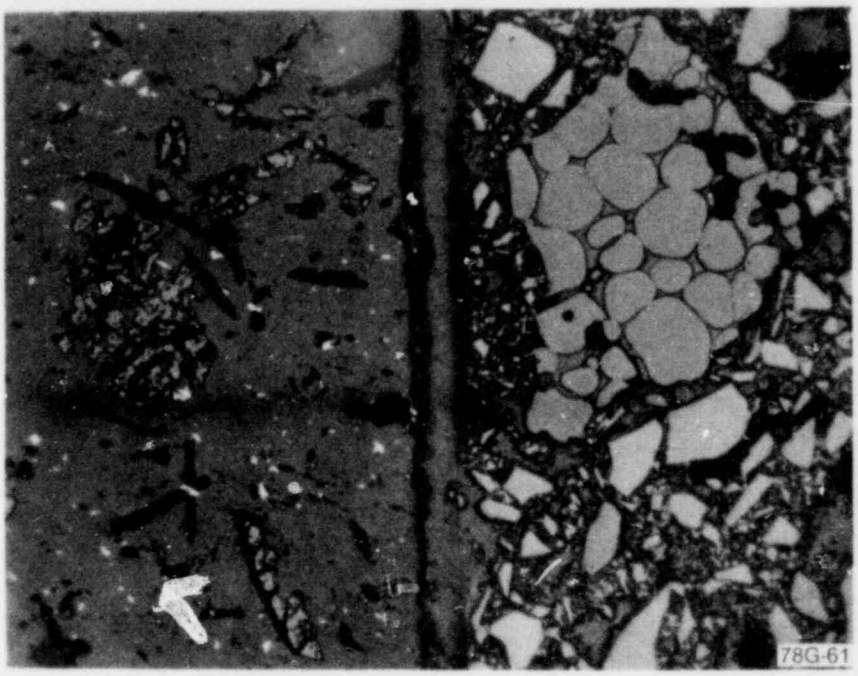

Figure F-3. Interface of ceramic disc with Sauereisen No. 8 after irradiation (200X).

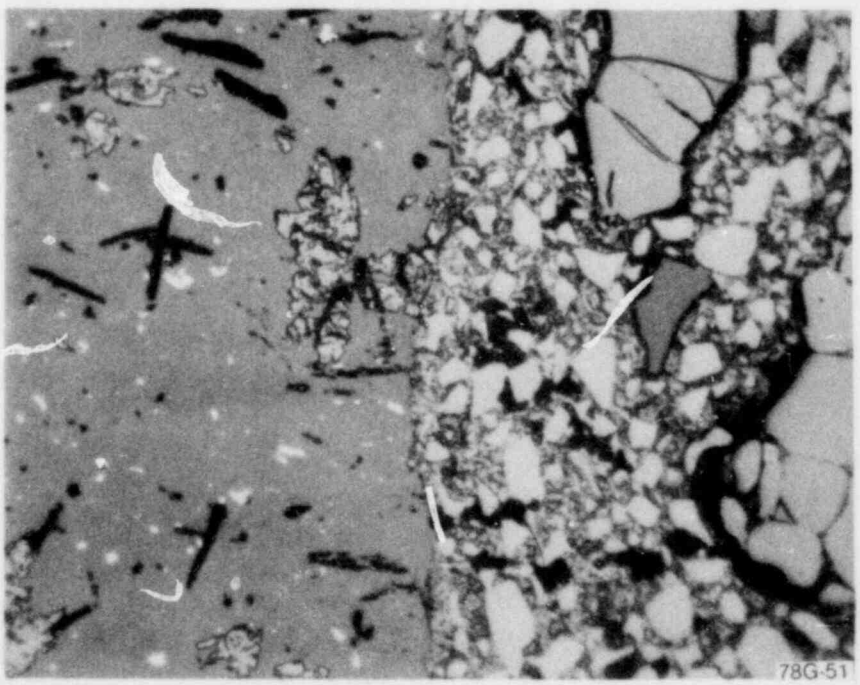

GS-017-005

Figure F-4. Interface of ceramic disc with Sauereisen No. 12 after irradiation (200X).

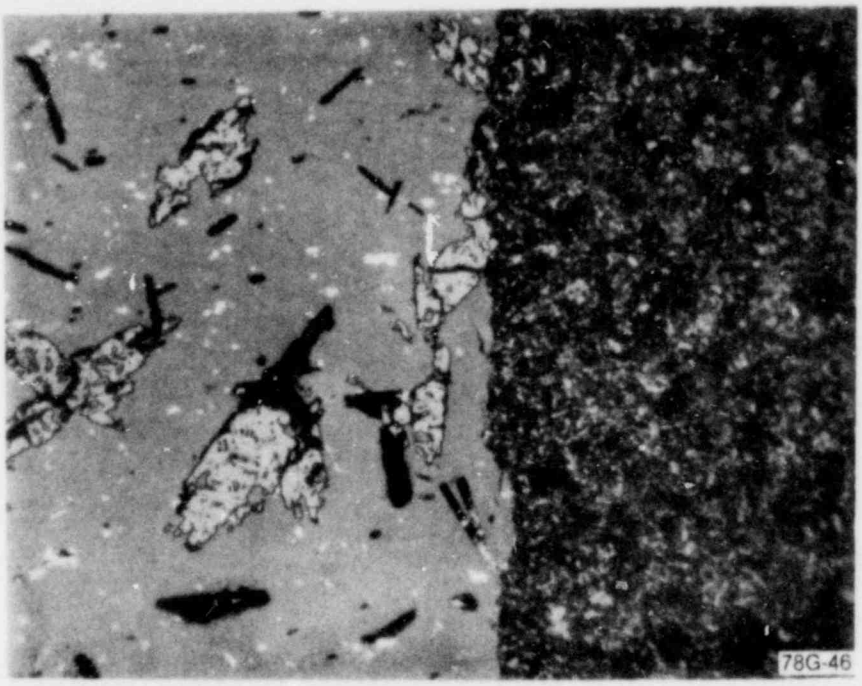

Figure F-5. Interface of ceramic disc with Ceramabond 503 after irradiation (200X).

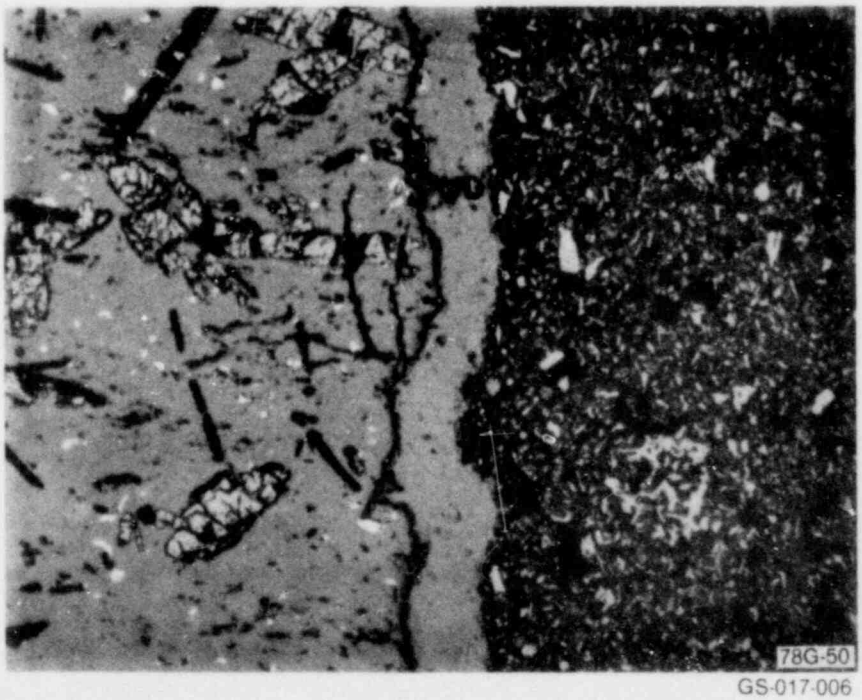

GS-017-006

Figure F-6. Interface of ceramic disc with Dylon C-7 after irradiation (200X).

Figure F-7. Interface of ceramic disc, Ceramabond 503, and Sauereisen No. 8 after irradiation (200X).

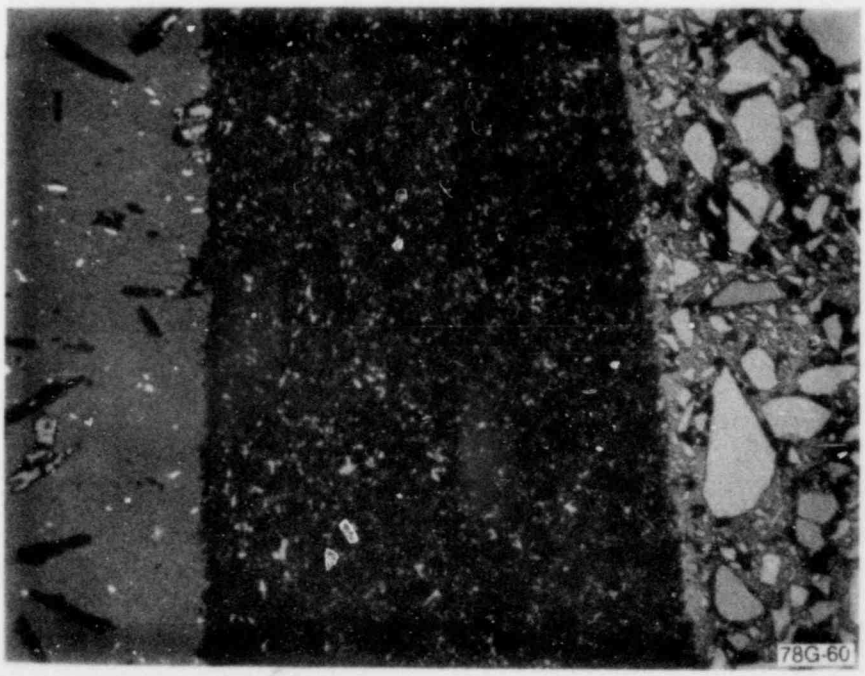

GS-017-007

Figure F-8. Interface of ceramic disc, Ceramabond 503, and Sauereisen No. 12 after irradiation (200X).

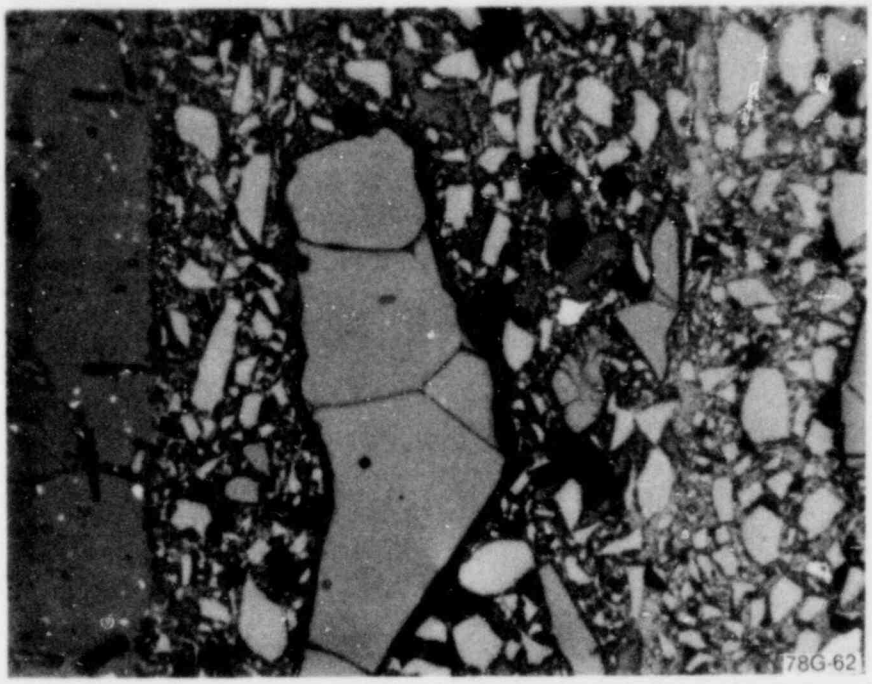

Figure F-9. Interface of ceramic disc, Sauereisen No. 8, and Sauereisen No. 12 after irradiation (200X).

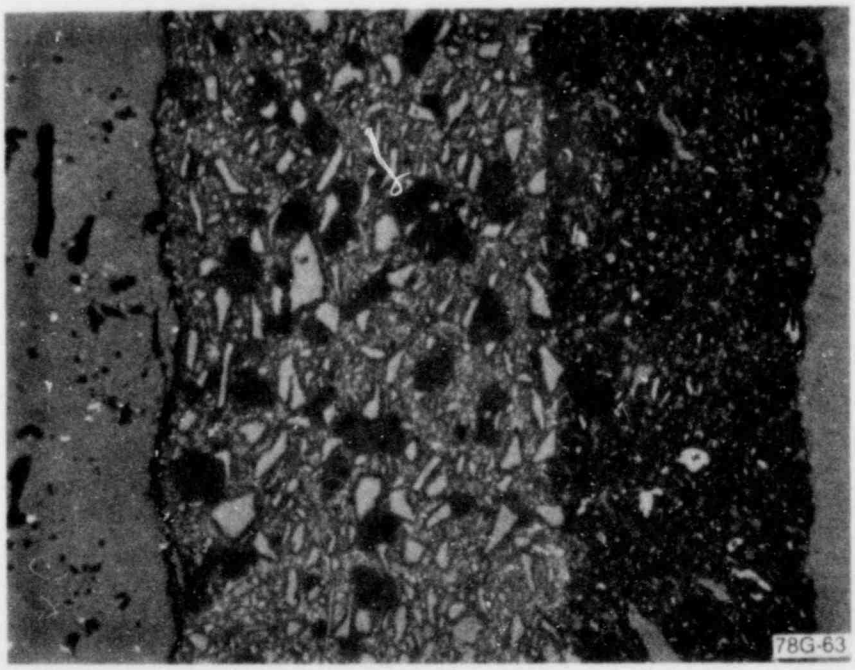

GS-017-008

Figure F-10. Interface of ceramic disc, Denex No. 2, and Dylon C-7 after irradiation (200X).

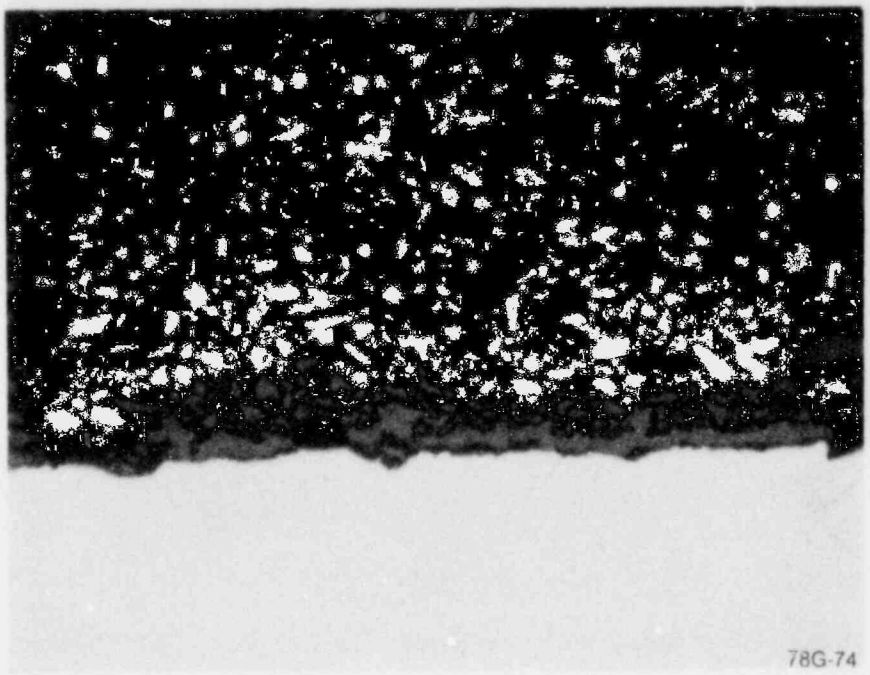

Figure F-11. Interface of 304 stainless steel disc with Yellow Cerro after irradiation (200X).

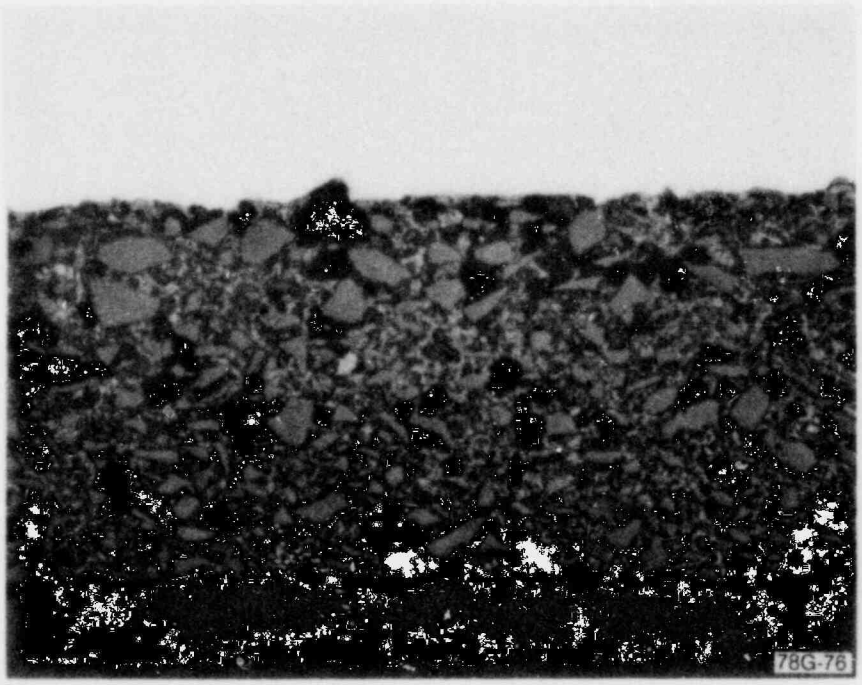

GS-017-009

Figure F-12. Interface of 304 stainless steel disc with Denex No. 2 after irradiation (200X).

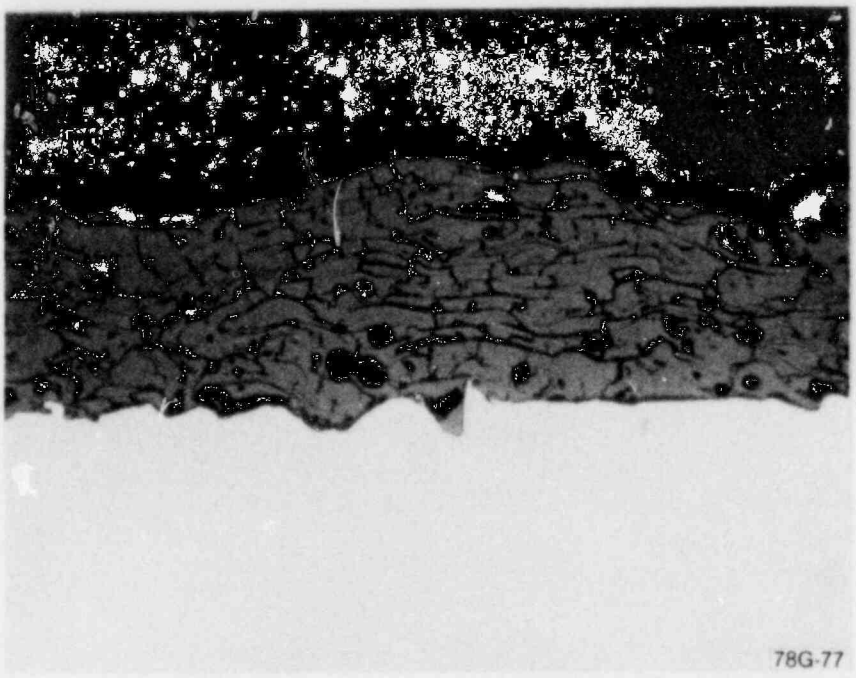

Figure F-13. Interface of 304 stainless steel disc with the Flame Sprayed ceramic after irradiation (200X).

Figure F-14. Interface of 304 stainless steel disc with Dylon C-7 after irradiation (200X).

APPENDIX G

PHOTOGRAPHS OF IRRADIATED TEST COILS

APPENDIX G

PHOTOGRAPHS OF IRRADIATED TEST COILS

The test coils were carefully removed from the test capsule and photographed before any additional test data was obtained. These photographs are shown in Figures G-1 through G-8.

Figure G-1. Irradiated coils prepared on ceramic forms using Alloy 406 wire and Yellow Cerro cement.

GS-017-0 '1

Figure G 2. Irradiated coils prepared on ceramic forms using Alloy 406 wire and Denex No. 2 cement. Three flux monitors are shown on one of the coils.

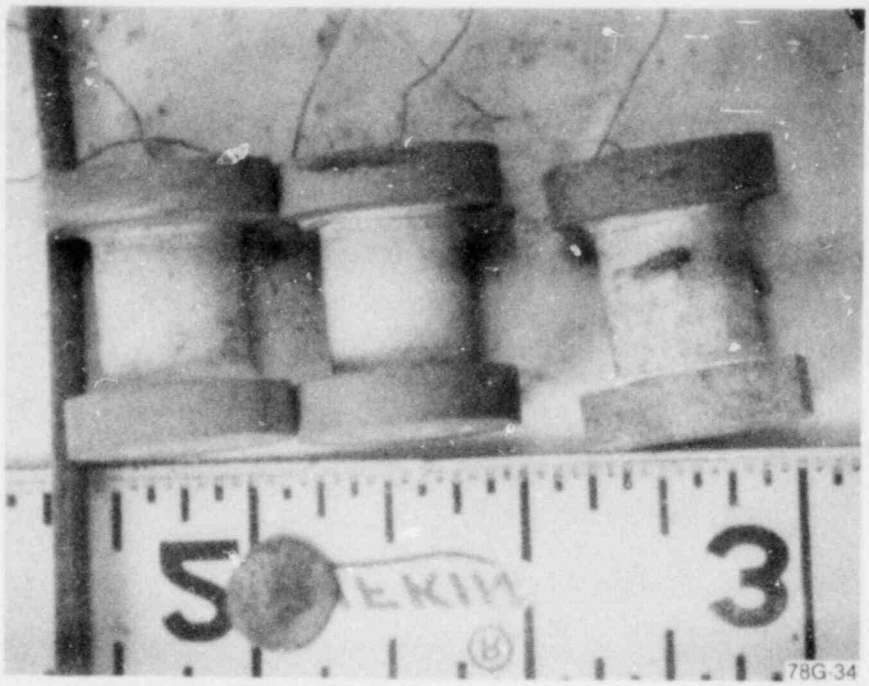

Figure G-3. Irradiated coils prepared on ceramic forms using Alloy 406 wire and Ceramabond 503 cement.

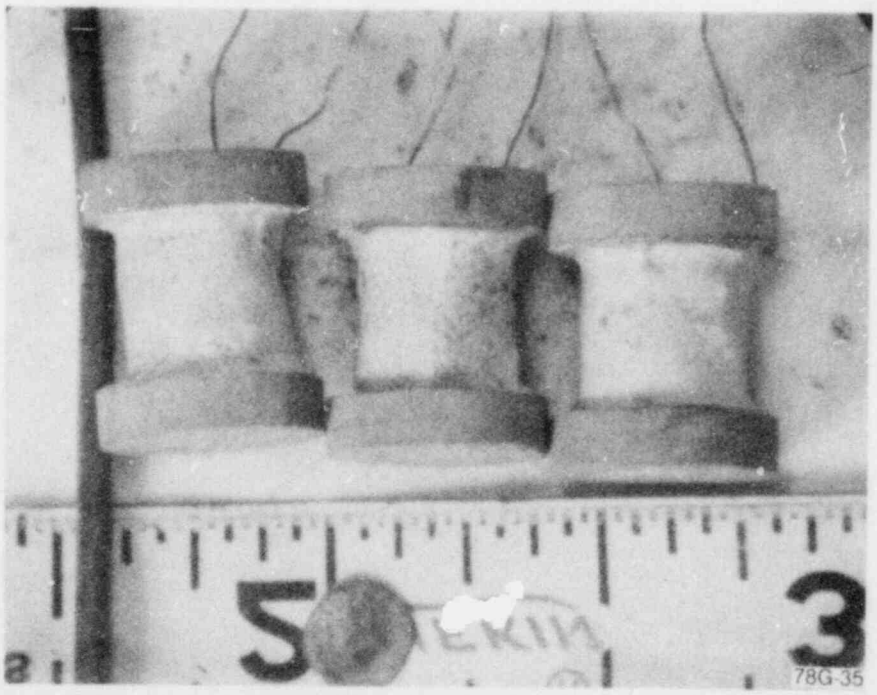

GS-017-012

Figure G-4. Irradiated coils prepared on ceramic forms using Alloy 406 wire with Ceramabond 503 (first coating) and Sauereisen No. 8 cements.

Figure G-5. Irradiated coils prepared on ceramic forms using Alloy 406 wire and Dylon C-7 cements.

GS-017-013

Figure G-6. Irradiated coils prepared on ceramic forms using platinum wire and Ceramabond 503 cement.

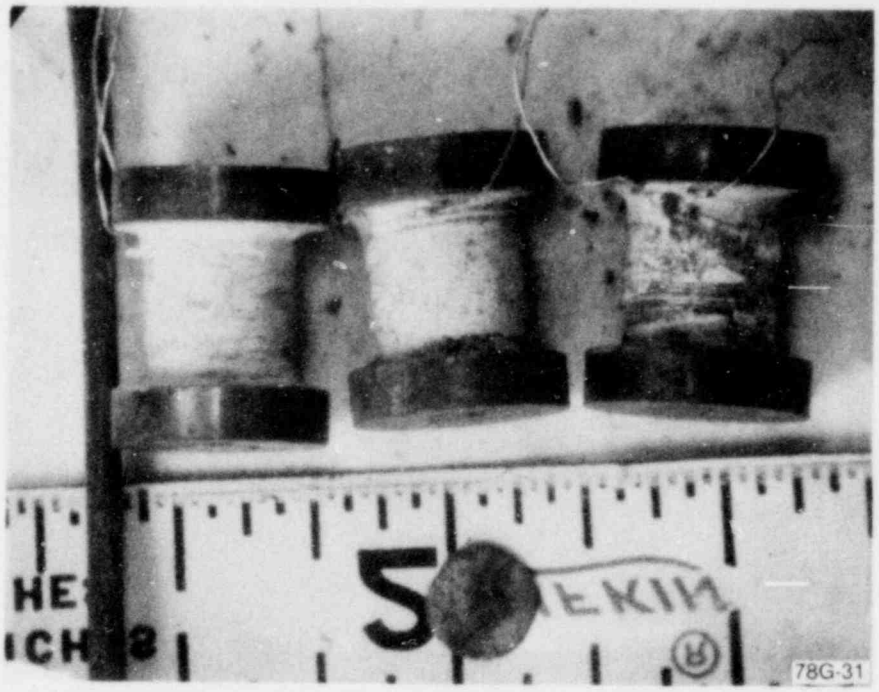

Figure G-7. Irradiated coils prepared on stainless steel coil form using Alloy 406 wire and Ceramabond 503 cement.

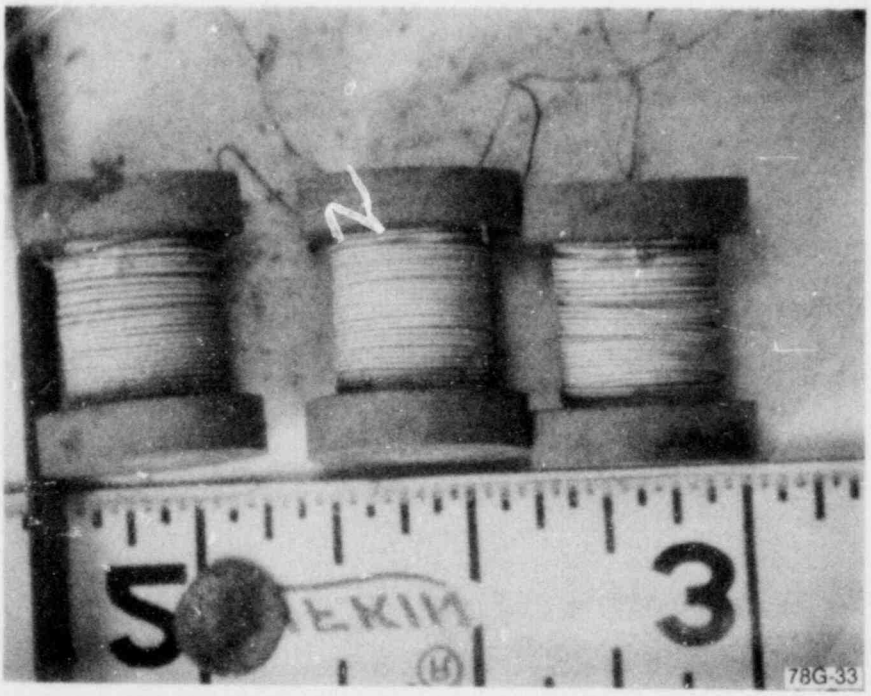

GS-017-014

Figure G-8. Irradiated bifilar wound coils on ceramic coil forms using Alloy 406 wire.

APPENDIX H

PHOTOMICROGRAPHS OF THE CERAMIC INSULATED WIRES

APPENDIX H

PHOTOMICROGRAPHS OF THE CERAMIC INSULATED WIRES

The test coils were mounted and sectioned by standard metallographic techniques before and after irradiation. Photomicrographs of the wire components of the coils are shown in Figures H-1 through H-6.

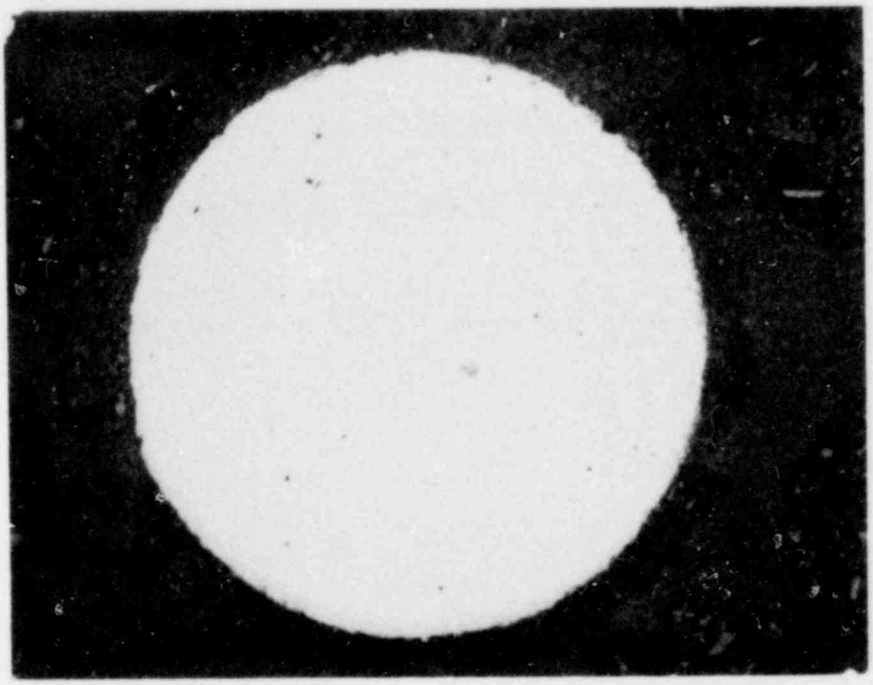

Figure H-1. Metallograph of unirradiated 406 Silver Alloy wire (400X).

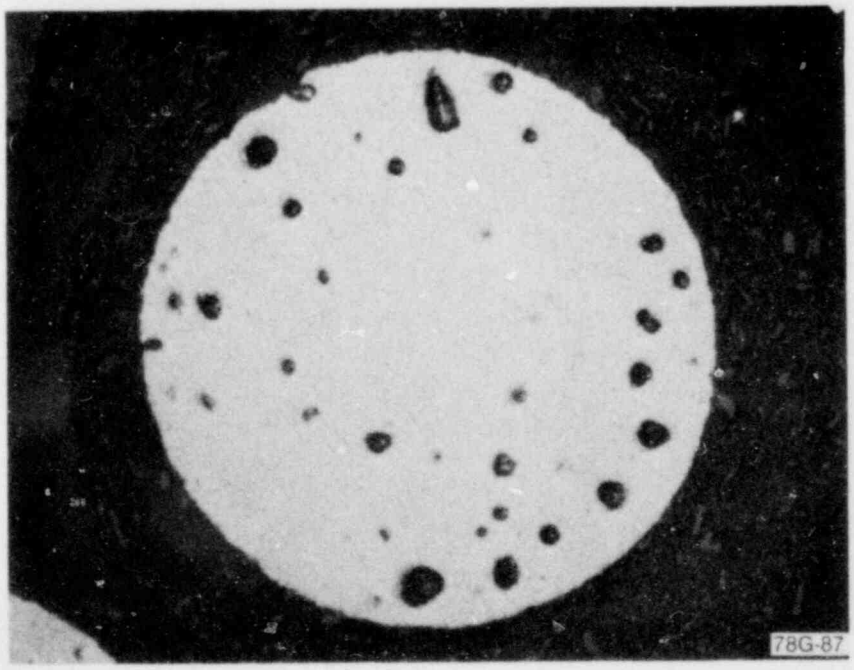

GS-017-015

Figure H-2. Metallograph of irradiated 406 Silver Alloy wire (400X).

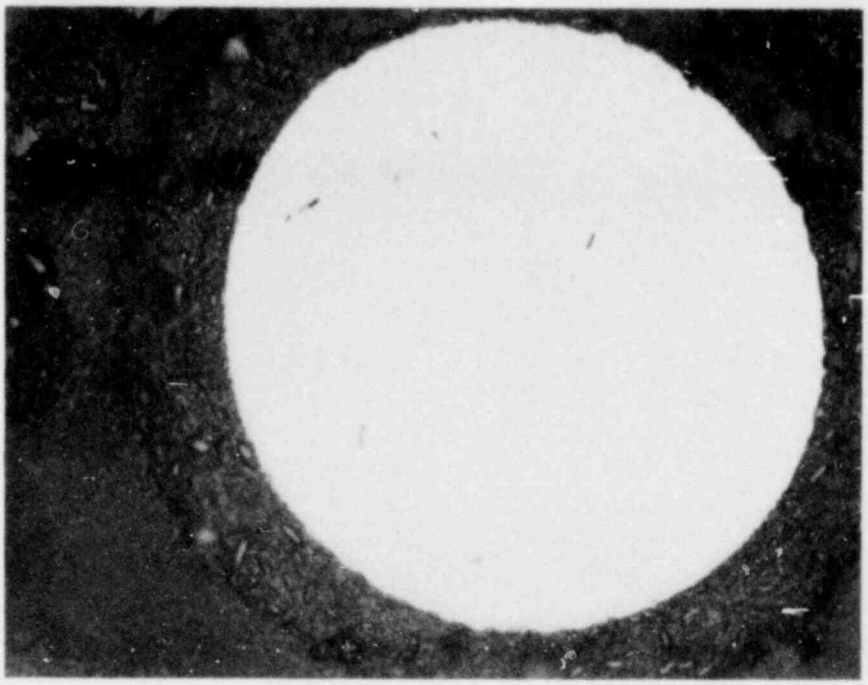

Figure H-3. Metallograph of unirradiated platinum wire (400X).

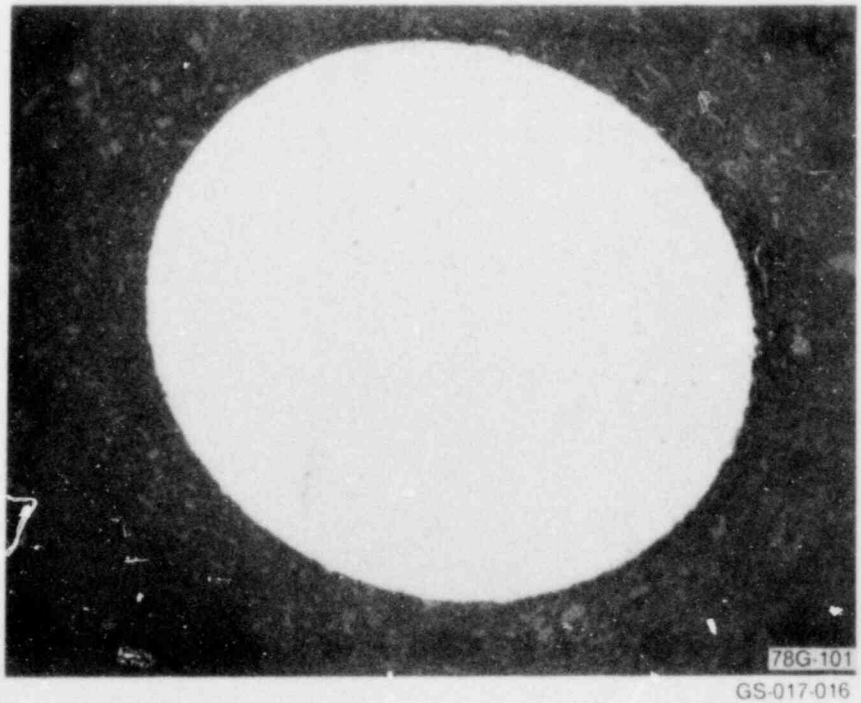

GS-017-016

Figure H-4. Metallograph of irradiated platinum wire (400X).

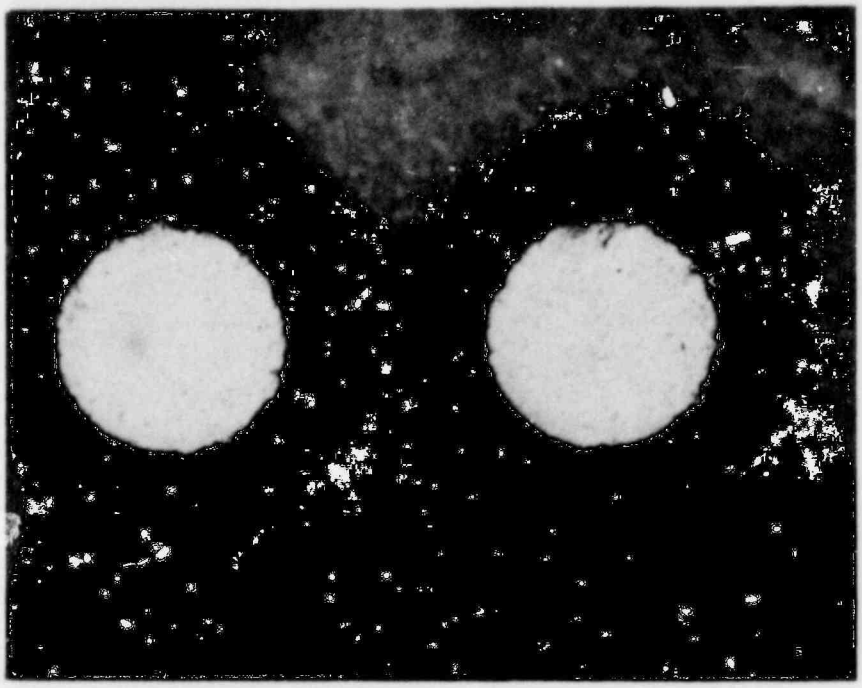

Figure H-5. Metallograph of unirradiated gold wire (600X).

GS-017-017

Figure H-6. Metallograph of irradiated gold wire (600X).